

Powder-Binder Separation during Powder Injection Molding

Bc. Daniel Sanétrník

Master thesis
2012



Tomas Bata University in Zlín
Faculty of Technology

Univerzita Tomáše Bati ve Zlíně

Fakulta technologická

Ústav fyziky a mater. inženýrství

akademický rok: 2011/2012

ZADÁNÍ DIPLOMOVÉ PRÁCE

(PROJEKTU, UMĚLECKÉHO DÍLA, UMĚLECKÉHO VÝKONU)

Jméno a příjmení: **Bc. Daniel SANÉTRNÍK**

Osobní číslo: **T10350**

Studijní program: **N 2808 Chemie a technologie materiálů**

Studijní obor: **Materiálové inženýrství**

Téma práce: **Separace materiálových komponentů při procesu
vstřikování práškových materiálů**

Zásady pro vypracování:

The aim of this master thesis is to describe a major quality-influencing factor in powder injection molding (PIM) – a phase separation. The theoretical part describes PIM technology in general, its advantages and disadvantages, PIM process and its main stages – feedstock preparations, injection molding, debinding and sintering. This part also focuses on a theoretical study of the phase separation. The second part is practical and consists of injection molding of various commercially available feedstock compositions on specially designed testing mold, and qualitative as well as quantitative observation of powder/binder separation employing SEM microscopy combined with EDX and simulation approaches.

Rozsah diplomové práce:

Rozsah příloh:

Forma zpracování diplomové práce: tištěná

Seznam odborné literatury:

1. R.M. German, Powder Injection Moulding. 1st Edn, Metal Powder Industries Federation, Princeton (1995)
2. HAUSNEROVÁ, B.: Powder Injection Moulding - An Alternative Processing Method for Automotive Items. Trends and Developments in Automotive Engineering, Vienna: InTech, p. 129-146 (2011)

Vedoucí diplomové práce:

prof. Ing. Berenika Hausnerová, Ph.D.

Ústav výrobního inženýrství

Datum zadání diplomové práce:

13. února 2012


Termín odevzdání diplomové práce:

7. května 2012

Ve Zlíně dne 13. února 2012


doc. Ing. Roman Čermák, Ph.D.
děkan




Mgr. Aleš Mráček, Ph.D.
ředitel ústavu

PROHLÁŠENÍ

Prohlašuji, že

- beru na vědomí, že odevzdáním diplomové/bakalářské práce souhlasím se zveřejněním své práce podle zákona č. 111/1998 Sb. o vysokých školách a o změně a doplnění dalších zákonů (zákon o vysokých školách), ve znění pozdějších právních předpisů, bez ohledu na výsledek obhajoby ¹⁾;
- beru na vědomí, že diplomová/bakalářská práce bude uložena v elektronické podobě v univerzitním informačním systému dostupná k nahlédnutí, že jeden výtisk diplomové/bakalářské práce bude uložen na příslušném ústavu Fakulty technologické UTB ve Zlíně a jeden výtisk bude uložen u vedoucího práce;
- byl/a jsem seznámen/a s tím, že na moji diplomovou/bakalářskou práci se plně vztahuje zákon č. 121/2000 Sb. o právu autorském, o právech souvisejících s právem autorským a o změně některých zákonů (autorský zákon) ve znění pozdějších právních předpisů, zejm. § 35 odst. 3 ²⁾;
- beru na vědomí, že podle § 60 ³⁾ odst. 1 autorského zákona má UTB ve Zlíně právo na uzavření licenční smlouvy o užití školního díla v rozsahu § 12 odst. 4 autorského zákona;
- beru na vědomí, že podle § 60 ³⁾ odst. 2 a 3 mohu užít své dílo – diplomovou/bakalářskou práci nebo poskytnout licenci k jejímu využití jen s předchozím písemným souhlasem Univerzity Tomáše Bati ve Zlíně, která je oprávněna v takovém případě ode mne požadovat přiměřený příspěvek na úhradu nákladů, které byly Univerzitou Tomáše Bati ve Zlíně na vytvoření díla vynaloženy (až do jejich skutečné výše);
- beru na vědomí, že pokud bylo k vypracování diplomové/bakalářské práce využito softwaru poskytnutého Univerzitou Tomáše Bati ve Zlíně nebo jinými subjekty pouze ke studijním a výzkumným účelům (tedy pouze k nekomerčnímu využití), nelze výsledky diplomové/bakalářské práce využít ke komerčním účelům;
- beru na vědomí, že pokud je výstupem diplomové/bakalářské práce jakýkoliv softwarový produkt, považují se za součást práce rovněž i zdrojové kódy, popř. soubory, ze kterých se projekt skládá. Neodevzdání této součásti může být důvodem k neobhájení práce.

Ve Zlíně 9.5.2012

.....

¹⁾ zákon č. 111/1998 Sb. o vysokých školách a o změně a doplnění dalších zákonů (zákon o vysokých školách), ve znění pozdějších právních předpisů, § 47 Zveřejňování závěrečných prací:

(1) Vysoká škola nevydělečně zveřejňuje disertační, diplomové, bakalářské a rigorózní práce, u kterých proběhla obhajoba, včetně posudků oponentů a výsledku obhajoby prostřednictvím databáze kvalifikačních prací, kterou spravuje. Způsob zveřejnění stanoví vnitřní předpis vysoké školy.

(2) Disertační, diplomové, bakalářské a rigorózní práce odevzdané uchazečem k obhajobě musí být též nejméně pět pracovních dnů před konáním obhajoby zveřejněny k nahlížení veřejnosti v místě určeném vnitřním předpisem vysoké školy nebo není-li tak určeno, v místě pracoviště vysoké školy, kde se má konat obhajoba práce. Každý si může ze zveřejněné práce pořizovat na své náklady výpisy, opisy nebo rozmnoženiny.

(3) Platí, že odevzdáním práce autor souhlasí se zveřejněním své práce podle tohoto zákona, bez ohledu na výsledek obhajoby.

²⁾ zákon č. 121/2000 Sb. o právu autorském, o právech souvisejících s právem autorským a o změně některých zákonů (autorský zákon) ve znění pozdějších právních předpisů, § 35 odst. 3:

(3) Do práva autorského také nezasahuje škola nebo školské či vzdělávací zařízení, užije-li nikoli za účelem přímého nebo nepřímého hospodářského nebo obchodního prospěchu k výuce nebo k vlastní potřebě dílo vytvořené žákem nebo studentem ke splnění školních nebo studijních povinností vyplývajících z jeho právního vztahu ke škole nebo školskému či vzdělávacímu zařízení (školní dílo).

³⁾ zákon č. 121/2000 Sb. o právu autorském, o právech souvisejících s právem autorským a o změně některých zákonů (autorský zákon) ve znění pozdějších právních předpisů, § 60 Školní dílo:

(1) Škola nebo školské či vzdělávací zařízení mají za obvyklých podmínek právo na uzavření licenční smlouvy o užití školního díla (§ 35 odst. 3). Odpírá-li autor takového díla udělit svolení bez vážného důvodu, mohou se tyto osoby domáhat nahrazení chybějícího projevu jeho vůle u soudu. Ustanovení § 35 odst. 3 zůstává nedotčeno.

(2) Není-li sjednáno jinak, může autor školního díla své dílo užít či poskytnout jinému licenci, není-li to v rozporu s oprávněnými zájmy školy nebo školského či vzdělávacího zařízení.

(3) Škola nebo školské či vzdělávací zařízení jsou oprávněny požadovat, aby jim autor školního díla z výdělku jím dosaženého v souvislosti s užitím díla či poskytnutím licence podle odstavce 2 přiměřeně přispěl na úhradu nákladů, které na vytvoření díla vynaložily, a to podle okolností až do jejich skutečné výše; přitom se přihlédne k výši výdělku dosaženého školou nebo školským či vzdělávacím zařízením z užití školního díla podle odstavce 1.

ABSTRACT

The aim of this master thesis is to describe a major quality-influencing factor in powder injection molding (PIM) - a phase separation. Separation of powder and binder components of a feedstock might cause visual defects and cracks on the final parts. In the theoretical part of the thesis, PIM process and its steps are described, and an overview of PIM applications is given. Also, current research on the phase separation is reviewed. In the experimental, injection molding of two commercially available feedstocks is performed on a testing mold specially designed to generate separation. Then, SEM microscopy combined with EDX analysis as well as quantitative evaluation of the separation were performed, and thus the feedstocks were compared.

Keywords: powder injection molding, phase separation, feedstock, scanning electron microscope (SEM), energy dispersive X-ray spectroscopy (EDX)

ABSTRAKT

Cílem diplomové práce je popis faktorů ovlivňujících kvalitu produktů vyrobených technologií vstřikování práškových materiálů, tzv. PIM. Hlavním problémem, který může způsobit vady finálního produktu, je separace materiálových komponent. Teoretická část popisuje PIM proces, jeho jednotlivé fáze (míchání, vstřikování, odstranění plniva a slinování) a aplikační možnosti. Dále je zde věnována pozornost teoretickému studiu separace fází. V praktické části je provedeno vstřikování dvou komerčně dostupných PIM materiálů na testovací formě. Tato forma byla navržena speciálně pro studium separace. Materiály jsou poté studovány pomocí SEM mikroskopie v kombinaci s EDX analýzou, jsou kvantitativně vyhodnoceny a porovnány.

Klíčová slova: vstřikování prášků, separace, komponent, elektronová mikroskopie (SEM), energiově disperzní rentgenová spektroskopie (EDX)

ACKNOWLEDGEMENTS

My grateful thanks belong to prof. Ing. Berenika Hausnerová, Ph.D. at Tomas Bata University in Zlín for many advices and consultations.

I would also like to thank doc. RNDr. Petr Ponižil, Ph.D. for his help with evaluation data and doc. Ing. Ivo Kuřitka, Ph.D. et Ph.D. for his help with TG analysis.

I hereby declare that the print version of my Bachelor's/Master's thesis and the electronic version of my thesis deposited in the IS/STAG system are identical.

Zlín 9th May 2012

.....

Daniel Sanétník

CONTENTS

INTRODUCTION	10
I THEORY	11
1 POWDER INJECTION MOLDING	12
1.1 APPLICATION OF PIM TECHNOLOGY	12
1.2 FEEDSTOCK FOR PIM	16
1.2.1 POWDERS FOR PIM	17
1.2.2 BINDERS FOR PIM	19
1.3 POWDER INJECTION MOLDING PROCESS	21
1.3.1 MIXING	23
1.3.2 INJECTION MOLDING	24
1.3.3 DEBINDING	25
1.3.4 SINTERING	29
1.3.5 FINAL PROCESSING	30
2 PHASE SEPARATION	31
2.1 QUALITY OF PIM FINAL PRODUCTS	31
2.2 RHEOLOGY OF PIM FEEDSTOCKS	32
2.3 HOMOGENEITY	35
2.4 EFFECT OF SHEAR RATE	36
2.5 MOLDABILITY	37
2.6 DESIGN OF A MOLD TESTING POWDER AND BINDER SEPARATION	41
II ANALYSIS	43
3 AIM OF THE MASTER THESIS	44
4 OPTIMIZATION OF INJECTION MOLDING PROCESS	45
4.1 INJECTION MOLDING MACHINE	45
4.2 FEEDSTOCK	46
4.3 INJECTION MOLDING PROCESS	47
5 SCANNING ELECTRON MICROSCOPY	49
5.1 SEM ANALYSIS OF FEEDSTOCKS	50
5.2 ENERGY DISPERSIVE X-RAY SPECTROSCOPY	55
5.2.1 EDX MAPPING	55
5.2.2 QUANTITATIVE X-RAY MAPPING	62
5.3 EVALUATION OF SEPARATION AND STATISTICS	64

CONCLUSION	69
BIBLIOGRAPHY	70
LIST OF ABBREVIATIONS	72
LIST OF FIGURES	73
LIST OF TABLES	75

INTRODUCTION

Powder injection molding (PIM) is a modern and effective way of processing metals and ceramics into the complex and precision products. The process combines traditional metallurgy and plastic molding. PIM process consists of several steps. The first step is mixing of metal/ceramic powder with polymer binder. The next step is injection molding, which is followed with the removal of binder from so called *green* part. Finally, a porous *brown* body is sintered to the final density. PIM parts have mechanical properties comparable to metallurgical products. Nowadays, the main issue of the technology is the powder/binder separation occurring during molding step. The phase separation causes problems such as surface defects, porosity, cracks and warpage detected on the final sintered parts. Due to the fact that the quality-failed parts are found at the end of the processing chain, for production efficiency it is very important to analyze/prevent separation during/after injection molding step, where the process is still reversible. Thus, the focus of this master thesis is to study phase separation in both qualitative and quantitative way.

I. THEORY

1 POWDER INJECTION MOLDING

1.1 Application of PIM technology

Powder injection molding (PIM) is a technological process for production of small, complex and precise shapes from metals (MIM) or ceramics (CIM). [1] The main advantage is that the PIM process combines the properties of polymers and metals. Polymers are cheap, available and they form to complex shapes, but on the other hand we need material properties which polymers cannot provide, e.g. high strength, corrosion, good electrical, thermal and optical properties. These properties have metals and ceramics. [2] Today's main use of PIM technology is the automotive, medicine, electronic and military industries. Some examples of products manufactured by PIM posted on Metal Powder Industries Federation [4] are listed below.

PIM technology was firstly used commercially in North America. Currently, Asia accounts for the dominant market position. The automotive has a share of 19.9 % in Japan. The European market in the automotive consumes PIM parts in more than 50 %. The first EU parts were manufactured in Germany. They were lock caps and lock shafts. Furthermore, they were fixing for cables, magnetic sensors, parts of camper van, cams for electrical adjustment mechanism of car seats and bonnet lock fixing bearings. The ceramics were employed for turbine wheels and large static components for automotive gas turbine program. Other parts produced in Europe since 2006 are glow plugs, gear wheels, valve sets and braking pads. [3]



Figure 1: MIM diesel turbocharger vane for automotive manufactured

by Fine Sinter Co. [4]

Automotive engine stator

PMG Füssen GmbH, Füssen, Germany, and its customer Schaeffler Group Automotive, Hirschaid, Germany, won the grand prize in the automotive engine category for a stator in a variable valve timing system in a 1.4 l engine. Made from a modified iron–copper PIM material, the complex part is formed to a density of 7.0 g/cm^3 . The stator, featuring five intricate center holes, is one-piece design replacing two parts. Very tight tolerances help to minimize any internal oil leakage between the adjoining pressurized chambers. The stator helps to reduce fuel consumption and the formation of exhaust gases as well as improves engine performance, especially torque at low rpm. It has two functions: spline for the timing-belt pulley and the VVT housing. The PIM processing offered substantial cost savings despite finishing operations such as sizing, machining, deburring, and steam treating. [4]



Figure 2: Automotive engine stator [4]

Stainless steel bobbins

ASCO Sintering Co., Commerce, California, and its customer Performance Friction Corp., Clover, S.C., won the award of distinction in the automotive chassis category for series of 316 stainless steel bobbins in a new braking system for race cars and high-performance vehicles. The two level part is available in 14 variations with eight or more bobbins in a single brake rotor assembly. The bobbins aid in tripling the brake-rotor fatigue life, reducing drag at elevated temperatures, as well as reducing vibration and temperature. The parts are made to a density of 7.0 g/cm^3 and have a tensile strength of 70,000 psi, yield strength of 45,000 psi, 13 % elongation, 48-foot-pound impact strength, and HRB 65. [4]



Figure 3: Stainless steel bobbins [4]

Stainless steel lock parts

Kinetics Climax Inc., Wilsonville, Oregon, won the award of distinction in the hardware/appliances category for three 17-4 PH stainless steel lockcylinder parts made by metal injection molding for Black & Decker Hardware and Home Improvement, Lake Forest, California. The MIM parts (locking bar, pin, and rack) operate in the Kwikset SmartKey lock cylinder, which contains one locking bar, five pins and five racks. The high-precision parts have a typical density of 7.7 g/cm^3 , and a typical tensile strength of 128,000 psi and typical yield strength of 100,000 psi. The complex PIM design provides significant cost savings and allows the consumer to rekey the lock easily without removing it or seeking a professional help. [4]



Figure 4: Stainless steel lock parts [4]

Hearing aid receiver can

FloMet LLC, Deland, Florida., and its customer, Starkey Laboratories Inc., Eden Prairie, Minnesota won the award of distinction in the electrical/electronic components category for a hearing aid receiver can made by metal injection molding. The thin-walled part is made of a nickel-iron-molybdenum alloy that provides the magnetic shunt effect required in the hearing aid to separate the internal receiver signal from the telecoil signal. The MIM part was previously deep drawn and required several interim annealing steps to achieve the necessary depth, in addition to forming the internal undercuts. Choosing the MIM manufacturing process provided 50 % cost saving over deep drawing as well as improved performance.



Figure 5: Hearing aid receiver can [4]

Orthodontic bracket

Flomet LLC, DeLand, Florida, and its customer Ormco Sybron Dental Specialties, Orange, California, won the Grand Prize for three parts - bracket, slide, and removable drop-in hook - used in the Damon 3MX self-ligation orthodontic tooth-positioning system. One bracket and one slide go on each tooth with a hook for about 5 % of the teeth. Very tiny, intricate parts are made by metal injection molding from 17-4 PH stainless steel powder to a density of 7.5 g/cm^3 . They have impressive physical properties: a tensile strength of 172,000 psi and yield strength of 158,000 psi. All of the parts are made to a net shape. The customer tumble polishes them and performs a brazing operation before assembly.



Figure 6 : Orthodontic bracket [4]

1.2 Feedstock for PIM

The attributes of the feedstock are determined by five factors:

- Powder characteristic
- Binder composition
- Powder:binder ratio
- Mixing method

Three possible situations of a feedstock powder:binder ratio are sketched in Figure 7.

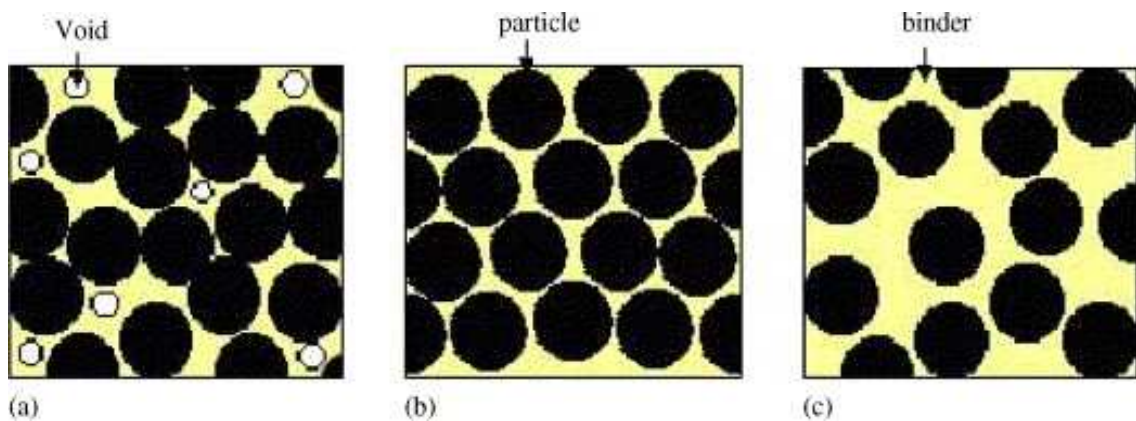


Figure 7: Three possible situations of powder:binder ratio in a feedstock;

a) excess of powder, b) critical, c) excess of binder [8]

- Excess of binder – binder separates from a powder during molding and causing slumping and other inhomogeneities in the final components. [5, 7]
- Excess of powder – results in a material with trapped voids, which during debinding cause cracking, and rather high viscosity. High viscosity limits processing and prevents proper mold filling. [5, 7]

- Critical solids loading – corresponds to the particles in close contact. Most manufacturers use a powder binder ratio slightly less than the critical solids loading to ease molding while maintaining product quality. [5, 7]

1.2.1 Powders for PIM

Many types of metals and ceramics are used in PIM ranging from iron and steels such as alloy steels, high speed steels, stainless steels, hard metals, titanium, super alloys, magnetic alloys e.t.c. Ceramic powders commonly used are Al_2O_3 , TiO_2 , ZrO_2 , silica graphite and boron nitride. Important properties of powders are particle size, particle size distribution and shape. Particle size of an ideal PIM powder is between 0.5 and 20 μm , distribution broad and shape is regular round. If the powder shape and size are changed, it can affect flow properties of the feedstock. The characteristics of ideal metal and ceramic powders used for PIM technologies are summarized bellow [5, 6, 10]:

- Particle size distribution should be wide and regular round shape is preferred for better flow behavior.
- Low explosion and toxicity hazards are desired as well.
- Typical particle size of commercially used powders is between 0.5 and 20 μm . Particle size is important for the sintering.
- Dense particles free of internal air pockets are preferred.
- Minimum segregation, clean particle surface and no agglomeration are essential.

These parameters are the result of a compromise between demands arising from particular PIM operations (mixing, molding, debinding, and sintering). Scanning electron microscope (SEM) is the best tool available for observing the structure of PIM feedstocks as depicted in Figure 8 showing commercial material Catamold[®] 316L.

Examples of powders and their applications are shown in Table 1.

Table 1: Examples of PIM powders [9]

Material Family	Applications	Specific Alloys	Specific Feature
Stainless Steel	Medical, Eletronic, Tools, Sporting Goods, Aerospace, Consumer Products	17-4PH	Strength, head treatable, processability
		316L	Corrosion resistance, elongation, processability
		410L, 420L, 440C	Hardness, wear resistance, head treatable
		430L	Magnetic response
Low Alloy Steels (heat treated)	Tools, Bearings, Races, Consumer Goods	2200	Magnetic
		2700	High nickel
		4605	
		8620	Case hardenable
		4140	
		52100	
Tool Steels (heat treated)	Wood and Metal, Cutting Tolls	M2	Low cost
		M4	Processability
		T15	High speed, processability
		M42	High speed, processability
		H13	
Titanium	Medical, Aerospace, Consumer Products	Ti	Ligh weight
		Ti-6Al-4V	Ligh weight, high strenght
		Cu	High termal and electrical conductivity
		W-Cu, Mo-Cu	High termal conductivity, low thermal expansion
Magnetic	Electronic, solenoids, armatures, relays	Fe-3%Si	
		Fe-50%Ni	
		Fe-50%Co	
Hardmetals	Cutting and Wear Applications	WC-5Co	Higher hardness
		WC-10Co	Higher toughness
Refractory Metals	High Temperature, High Density, Eletronic	Ta	Electronic
		W-Ni-Cu, W-Ni-Fe	High density
Ceramics	Wear applications, Nozzles, Ferules	Alumina	Low cost
		Zirconia	High wear resistance
		Silicon Carbide	High wear resistance
		Silicon Nitrate	High performance

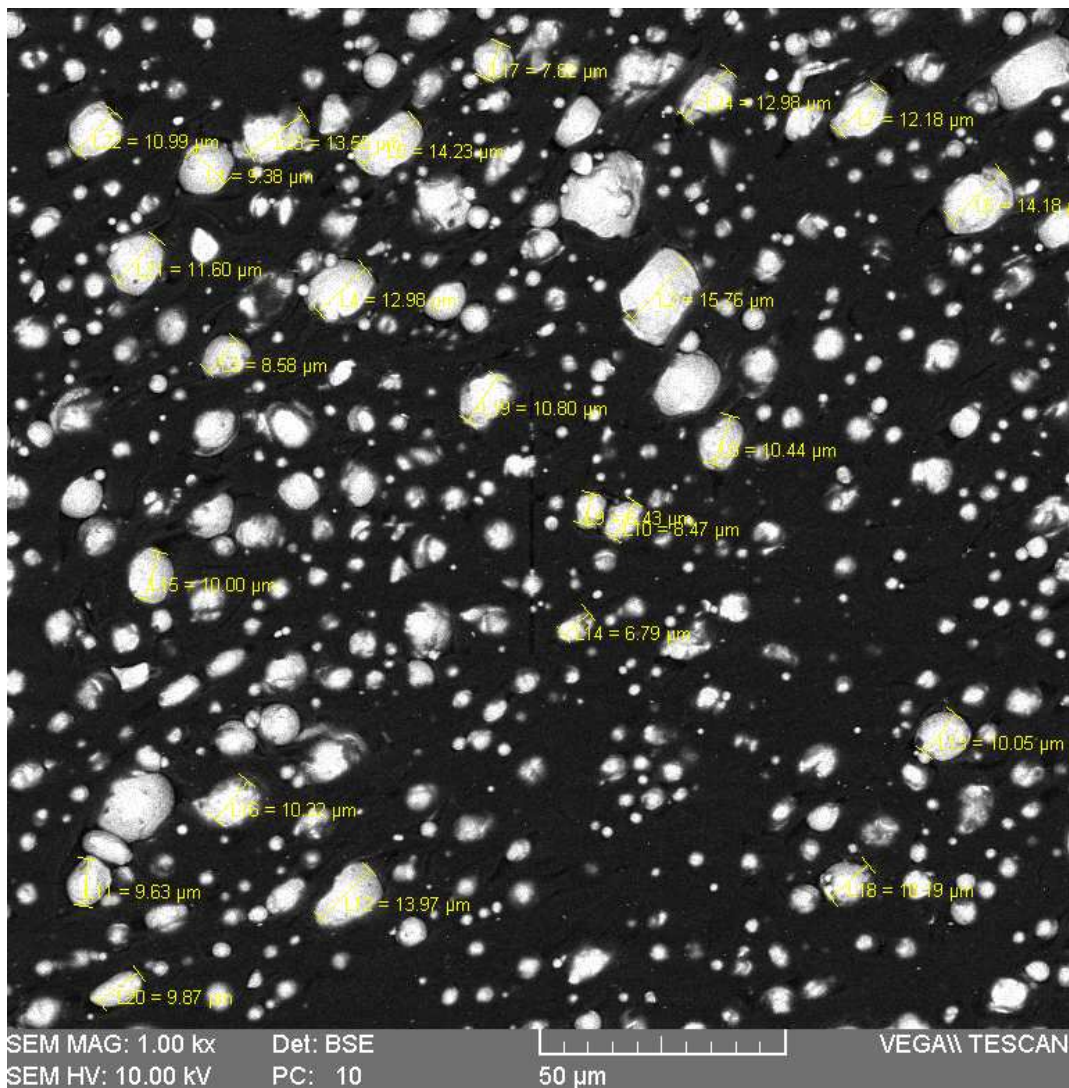


Figure 8: SEM of a feedstock used in PIM

1.2.2 Binders for PIM

Binder is the second component of a PIM feedstock. Two main functions of binders are lubricating particles during injection molding and holding them in the desired shape before sintering. Until the beginning of sintering binder is step wise removed/debinder from the molded part. Most binders systems consist of three parts:

- Main ingredient (paraffin, carnauba, palm oil, POM, PEG, PVA, water, epoxy, e.t.c.)
- Polymer backbone (e.g. PE, PP, PS, PMMA, methyl cellulose)
- Additive (stearic acid, oleic acid, glycerin, butyl stearate)

Examples of polymer binders are shown in Figure 9.

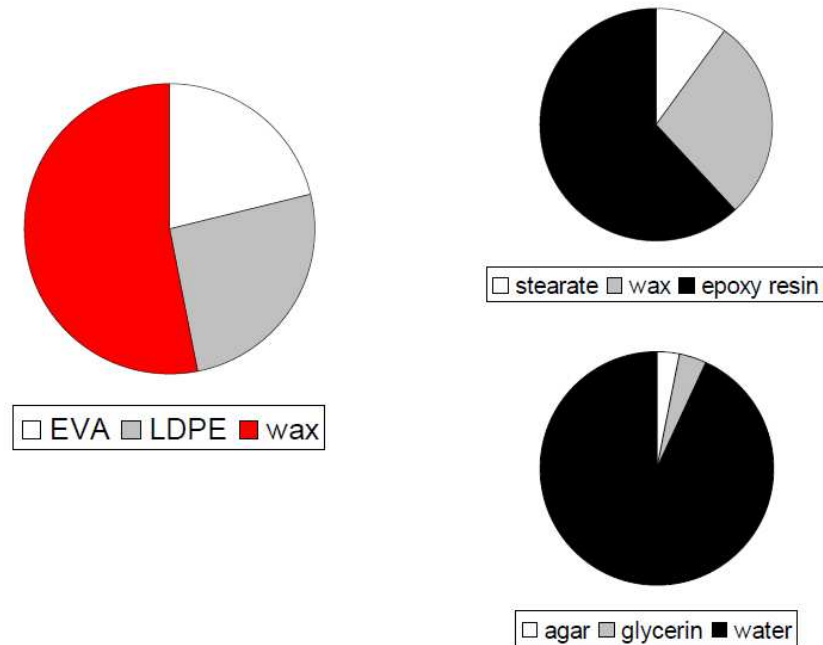


Figure 9: Polymer binders [12]

Main ingredients provide a coherence between binder and powder, but also lubricate system and facilitate the first phase of debinding. The backbone component provides a strength. Additives including dispersants, stabilizers, plasticizers and inter-molecular lubricants are employed to improve flow properties. Binders for PIM can be divided into two basic groups: wax-based, sometimes also called wax/polymer because one or more waxes are modified by polymer. The second group is polymer-based (polymer/polymer) consisted of blends of two or more polymers. [5, 11]

Two general forms of polymers are thermoplastic and thermosetting. Thermosets crosslink by heating when injection molded. The drawback of thermosets is that they cannot be reused (due to nonreversible crosslinking), and thus they are economically disadvantageous due to the high price of a feedstock. Therefore, the majority of PIM binders are thermoplastic. The most useful commercial polymers are polyethylene, polypropylene, polystyrene and wax. A prospective wax/polymer binder was recently designed by Marčíková [26]. It consists 20 % polyethylene, 20 % paraffin wax, 59 % polyethylene glycols (specifically: 10 % PEG1000, 39 % PEG4000 and 10 % PEG6000) and 1 % stearic

acid. The most successful polymer/polymer binders are polyacetal and water-soluble ones. Polyacetal binders provide excellent shape retention. Debinding is performed in highly concentrated nitric or oxalic acid. Because of this producers are concerned in health and safety regulations. Polyacetal binders are manufactured by BASF under the Catamold® trademark. Water-soluble binders were developed to replace wax/polymer binders, which often show low green strength, poor shape retention during debinding, use of environmentally hazardous solvents, and rather narrow processing windows. Such binders consist hydrophilic polyethylene oxide or polyvinyl alcohol. [6, 11]

PIM feedstock usually consists of around 40 vol. % of a binder system. The content might vary according to the characteristics of a powder used. After molding binders are extracted by several methods – solvent, thermal, catalytic or supercritical. [5, 6]

1.3 Powder injection molding process

PIM process can be divided into four basic steps:

- Mixing
- Injection molding
- Debinding
- Sintering

Figure 10 shows a scheme of the particular steps involved in PIM forming. In the first step, a binder is mixed with metal or ceramic powder. Homogeneous feedstock is then molded on an injection molding machine. Further, binder is removed from the component by debinding approach. The final step is sintering. Sintering bonds the particles together and a product density dramatically increases. [5, 6]

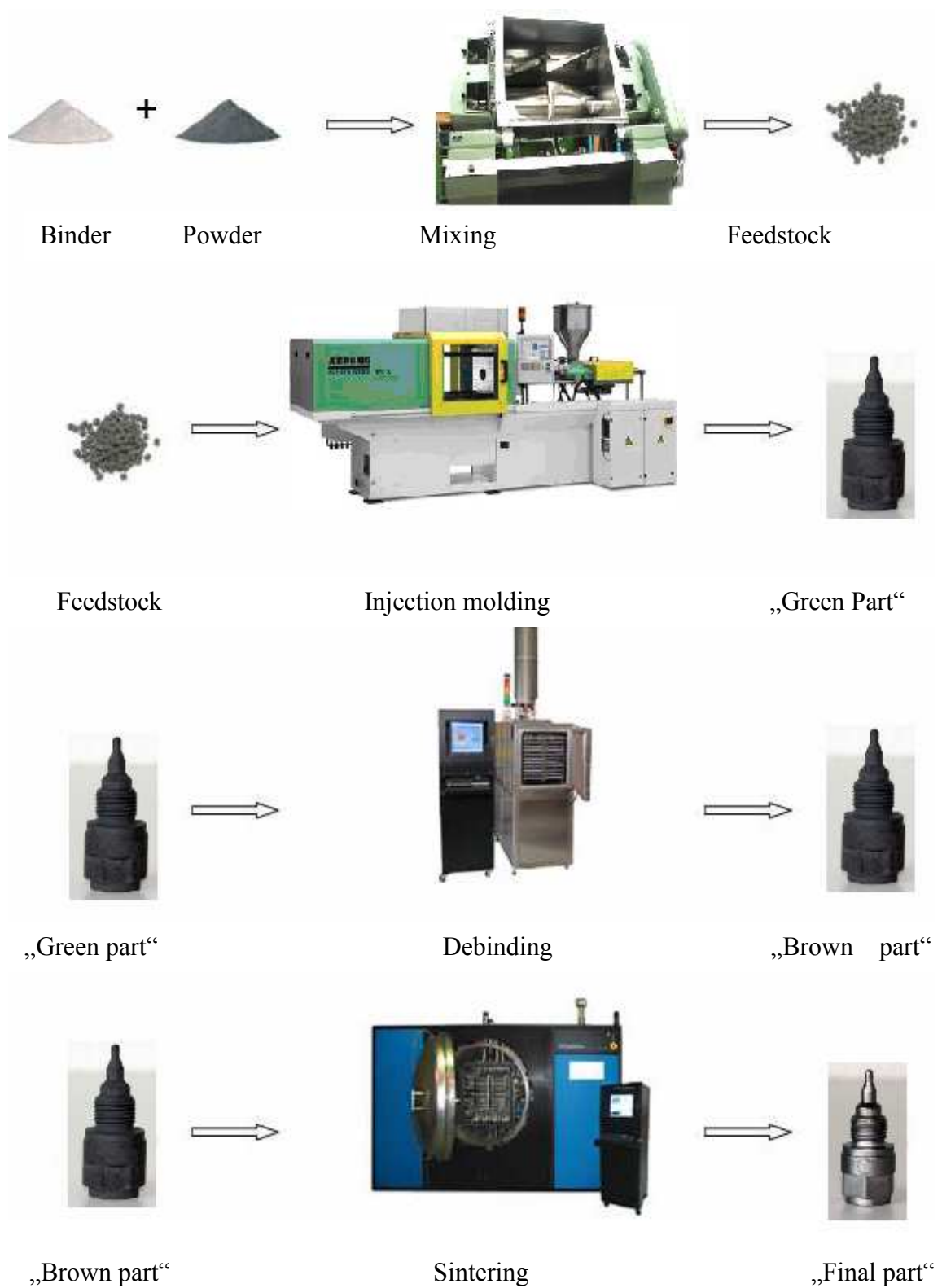


Figure 10: Schematic diagram of PIM [6]

1.3.1 Mixing

Mixing of feedstock is a critical step in PIM process. Weaknesses resulting from the mixing cannot be removed in further processing. Feedstock must be homogeneous with minimal segregations, no agglomerations and free of voids. All mixing deficiencies cause imperfections and deformations after sintering. The main factors affecting the quality of mixing are time, temperature, sequence of material addition, powder characteristic, formulation of binder, shear rate, and powder loading. [13] According to the type of binder mixing temperature varies from 80 to 200 °C and it takes several hours. For batch mixing (discontinuous) planetary mixers or Z-blades mixers are the most often used (Figure 11). Continuous homogenization of feedstocks is performed on extruders. The main factors influencing the use of discontinuous or continuous mixing are capacity, homogeneity and price. [6, 12] Nowadays, we use several methods to determine the quality of mixing, especially the critical solids loading of a powder/binder system. Most important is the measurement of density, melt flow, mixing torque or viscosity versus composition. The feedstocks are granulated or pelletized after mixing. [5]

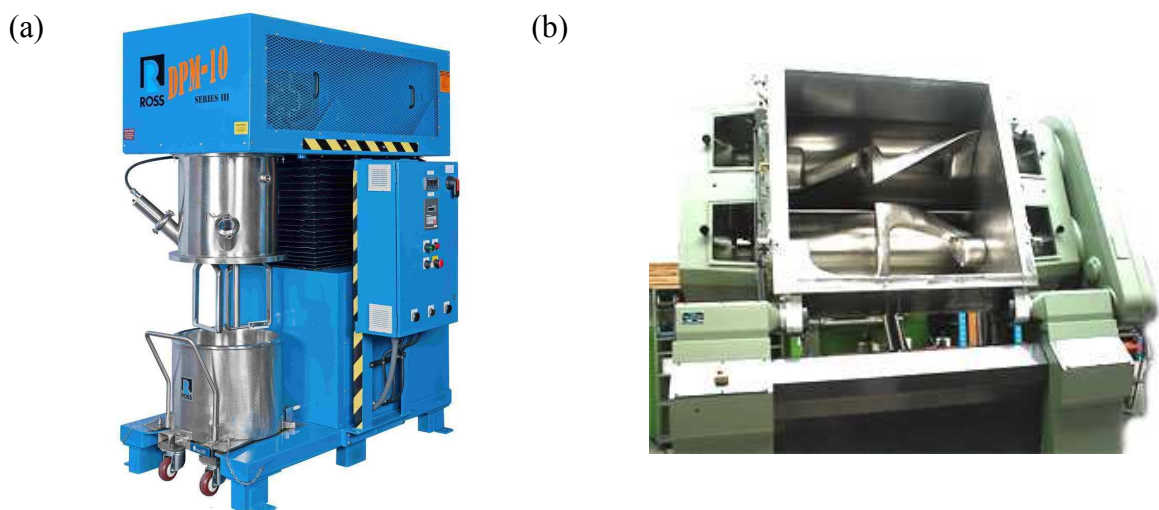


Figure 11: A batch mixing: (a) planetary mixer; (b) Z-blade mixer [14, 15]

1.3.2 Injection molding

MIM/CIM technology employs injection molding machines for plastics modified for processing of metal or ceramic powders. To reduce wear hardened screws and barrels are used, especially adapted screw geometry is designed to ensure homogeneity of highly filled compounds.

This process leads to the conversion of feedstock into a shape of the part. Granulated feedstock is fed into the barrel of the machine and heated to produce a semi-fluid mass. Then, the feedstock is injected by a force into the mold cavity through a gated runner system. Typical temperature used in the injection of polymer-based materials and wax-based material is 100 – 200 °C and they are injected using pressures between 50 and 150 MPa. [6, 16]

Injection unit consists of four main parts – hopper, reciprocating screw, heated barrel and nozzle. A standard injection molding cycle consists of five basic steps. First, material is fulfilled to the hopper of an injection molding machine. The second step is dosage. Feedstocks are melted in the plasticizing unit by heat and shear. The next step is the high pressure injection of material into the mold. When the sample is cooled, plasticizing unit splits off from the mold. The mold unit opens and the molded part is ejected by machine ejector system automatically. In some cases, a robotic system is integrated to remove fragile parts from the mold. [18]

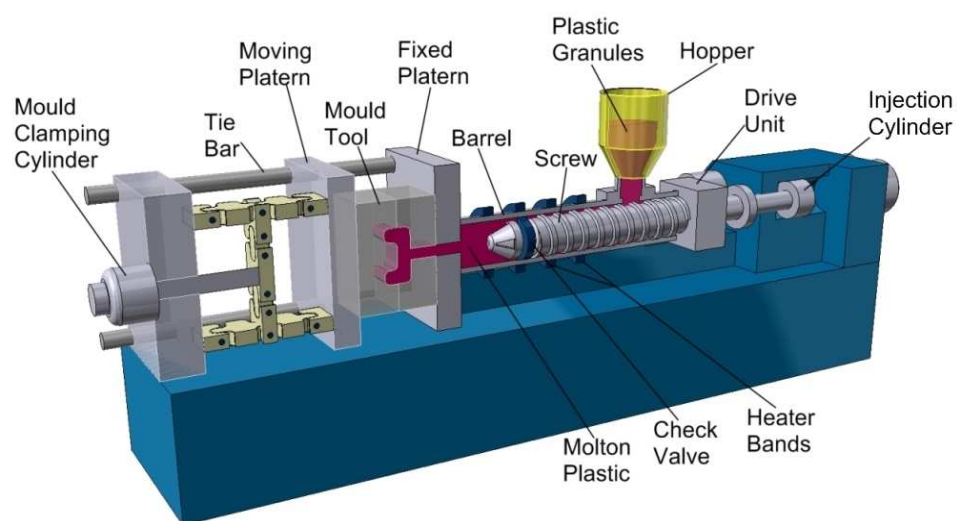


Figure 12: Injection molding machine [17]

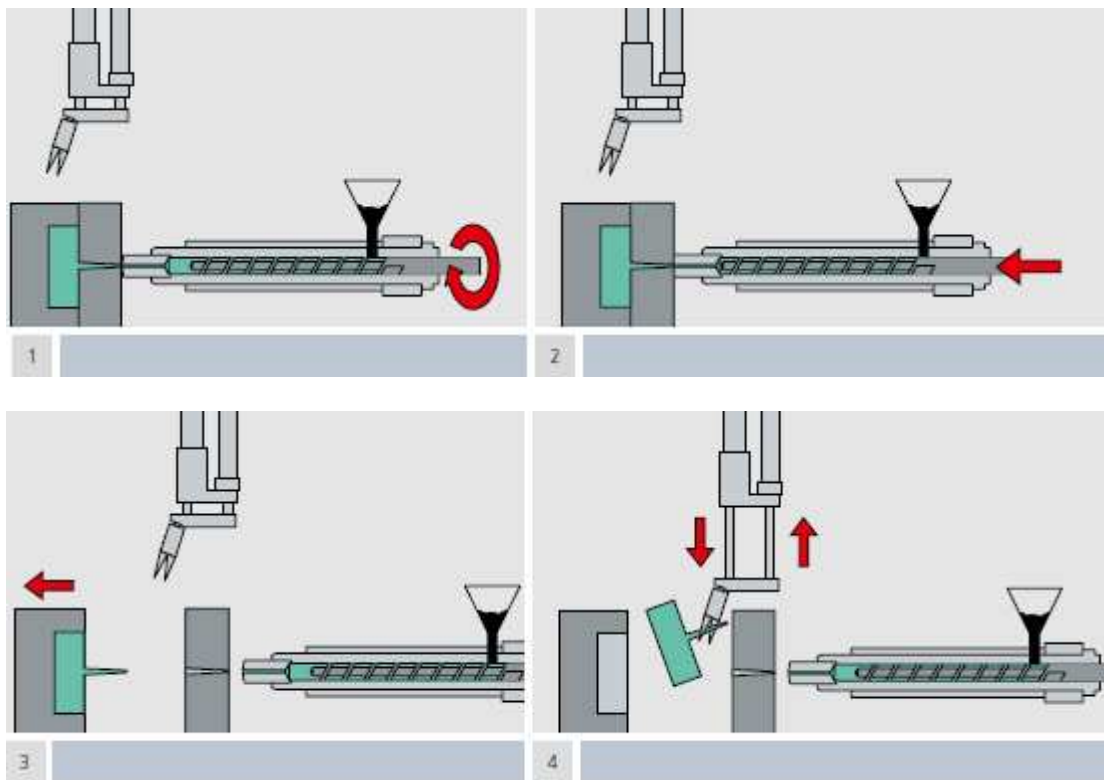


Figure 13: Scheme of a molding cycle [18]

Very important is the size and shape of the mold. The mold cavity dimensions must be up to 20 % than those of the final product. Exact magnification value depends on powder:binder ratio. This is due to shrinkage that occurs during sintering process. The mold design must meet several important parameters. These parameters affect product quality. The wall thickness should be minimal and uniform. This will not only speed up the time debinding and sintering, but also saves the consumption of material.

1.3.3 Debinding

In this step, binders are removed from molded products with the help of solvent or high temperature. Therefore, two main techniques are discerned - solvent and thermal debinding. Additionally, there are other methods combining these basic processes. Binder system determines the method that is selected for debinding. The product resulting from debinding is called *brown part*. At this stage it is very brittle and rather porous.

Thermal debinding

Most frequently used debinding method is the removal of binders with applied heat, either by degradation, evaporation or liquid extraction using a wicking material in contact with the debinded part. Thermal debinding is controlled via temperature profile. The binder is removed at atmospheric pressure and the presence of gas (nitrogen, hydrogen, argon or air). When the binder:powder ratio is chosen properly, binder will firstly evaporate from the component surface. Gradually the pores are formed which are increasingly larger. For this reason, the speed of heating gradually decreases. When the pores are unacceptable large or linked to each other, it can lead to cracks in the final part. This is the reason why the mixture of powder and binder must be homogeneous and separation of powder and binder during molding avoided.

During debinding a binder may melt by heat, and in the liquid state then flows out. With increasing temperature binder viscosity is reduced, and the flow is accelerated. The other possibility is that binder is not melted, but decomposed into low molecular weight species (such as water, methane, carbon dioxide or carbon monoxide). In such a case these elements are evaporated from the pores. When pores are sufficiently large, atmospheric pressure is used. If the resulting pores are too small to escape the vapors, reduced pressure must be employed.

The course of thermal debinding can be seen in Figure 14. [10]

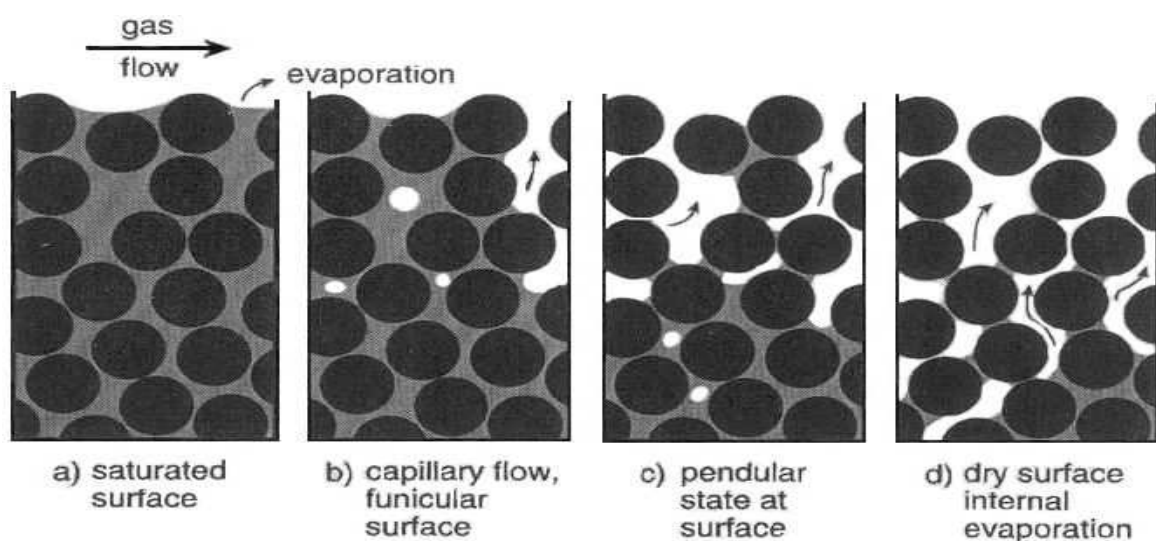


Figure 14 : Course of thermal debinding [5]

Solvent debinding

During solvent debinding, *green* part is immersed into the solvent that dissolves a particular component of a binder, except of the polymer backbone. Molded part is usually preheated to 40 – 80 °C, and then immersed in the solvent for several hours. Solvent extraction is widely employed for oil-polymer binder systems. The solvent is selected to dissolve the oil but not the polymer.

A similar method is debinding by a solvent vapor. Processing is performed in a protective enclosure at temperatures between 50 and 70 °C for times up to a day. Binder is extracted by vapor and removed from the system. Reactors include distillation section, where the binder is removed from the solvent. Then, the purified solvent is returned back to the cycle. [6, 10]

Most used solvents include:

- Solvents for immersion: ethylene dichloride, heptane or trichloroethane
- Debinding by solvent: vapour carbon tetrachloride, methyl ethyl ketone, hexane, heptane

Supercritical debinding

Supercritical binder removal is still not widely commercialized. There might occur problems with high pressures and heating the solvent as well as hindrances connected with high cost of equipment and long processing time. The sample and the solvent are heated and pressurized to the point when solvent starts to behave supercritical. i.e. it is vapor and liquid the same time. During the supercritical debinding there is not surface energy between liquid and vapor. Also, there are no changes in binder volume. The advantage of supercritical debinding is also lower temperatures, because high temperatures can damage the sample. The most common solvents are carbon dioxide, freon and propane. Commonly used

pressure and temperature during supercritical process are around 20 MPa and below 100 °C. [5, 10]

Catalytic debinding

In 1991, BASF introduced a new binder/debinding system for powder injection molding, which is commercialized as ready-to-mold metal and ceramic feedstock. The BASF process is a process characterized by a polyacetal based binder and an acid catalysed debinding technique. This process combines thermal and solvent debinding. Vapors of catalyst penetrate into emerging pores. The reaction depends on the speed of penetration of the catalyst into the pores and the decomposition of binders from pores. Typical conditions used are nitrogen atmosphere, atmospheric pressure and temperature of about 120 °C. Speed of debinding is constant around 2 mm/hour. Nitric acid is anhydrous and does not react with most PIM powders. The shape of the sample during the debinding does not change because the used temperature is below the melting temperature of a binder. [6, 10]

Water-soluble debinding

The most common solvent is water. This solvent can be used for water-soluble polymers. These are mostly polyethylene glycols, polyethylene oxide, polyvinyl alcohol, starches and polyacrylamide. These polymers are hydrophilic, because they contain atoms of oxygen or nitrogen. This makes water an appropriate solvent. The benefit of using water is that it is health safety. Other solvents may be flammable, toxic or even carcinogenic. Also, removal speed is much higher than that during thermal debinding. [6, 10]

On the base of a sample with a cross section thickness of 10 mm, containing powder having a particle size of 5 mm and solid loading of 60 vol. %, the different debinding techniques and times are compared in Table 2.

Table 2: Comparison of debinding techniques and times [5]

Binder system	Debinding technique	Conditions	Time in hours
Wax-polypropylene	Oxidation	Slow heat 150 °C, hold, heat to 600 °C in air	60
Wax-polyethylene	Wicking	Slow heat 350 °C, hold, heat to 750 °C in hydrogen	6
Wax-polymer	Supercritical	Heat in freon vapour at 10 °C/min to 600 °C under 10 MPa pressure	6
Wax-polyethylene	Vacuum extraction	Slow heat while passing low pressure, gas over compacts, heats to sintering temperature	36
Water-gel	Vacuum sublime or freeze dry	Hold in vacuum to extract water vapor from ice	8
Oil-polymer	Solvents immersion	Hold in ethylene dichloride at 50 °C	6
Water-gel	Air drying	Hold at 60 °C	10
Polyacetal-polyethylene	Catalytic debinding	Heat in nitric acid vapor 150 °C	6

1.3.4 Sintering

Sintering is a thermal process in which individual particles of a powder are welded together. This stage creates the final strength of the product. The process takes place in the furnaces with the protection atmosphere or in vacuum, using temperature below the melting temperature of metal. The composition of the atmosphere depends on the powder. Sintering in PIM technology is easier than in conventional metallurgy, because of the fact that in PIM technology finer powder is used. This will increase the surface energy of part. During the

sintering shrinkage occurs up to 20 %, because of the porosity due to the binder removal. Sintering temperature must be well controlled. [19, 20]

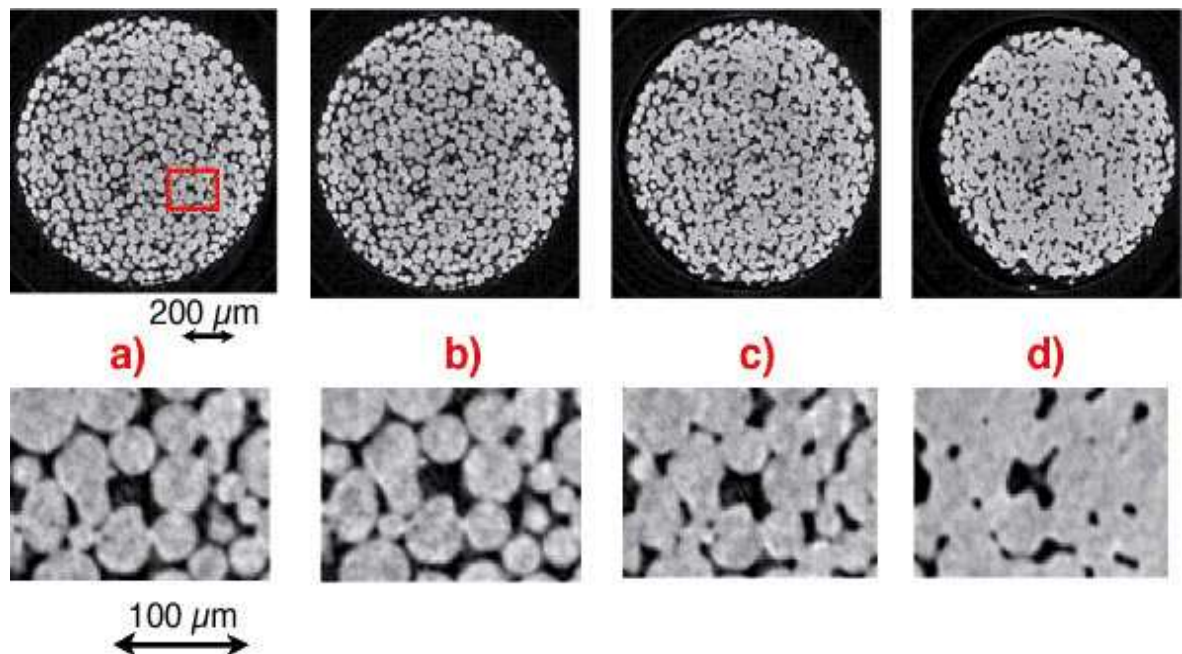


Figure 15: Sintering process

1.3.5 Final processing

Most of the PIM parts are completed after sintering process. However, some products are inspected, painted or wrapped after sintering. They can also be treated by conventional metallurgical processes, e.g. hot isostatic pressing to increase the density of sintered parts. The completed part is finally mounted to the machine or distributed. [4, 5]

2 PHASE SEPARATION

2.1 Quality of PIM final products

PIM is still a developing technology. There is much to explore to improve the quality of the final products. With many stages of the process - feedstock mixing, injection molding, debinding and sintering, more problems may arise than during traditional metallurgical production. [6]

Due to the composition of highly filled materials employed, it is natural that they have complex rheological properties. This can cause phase separation between the components of a feedstock, since the factor initiating the separation is high shear force/deformation during the mould filling process. It is supposed that a separated polymer film is formed on the mould surface.

Viscosity of a feedstock is also very important. Low viscosity causes disturbances during debinding, because the material has not sufficient strength and deforms during molding. On the other hand, too high viscosity causes problems during injection molding. Changes in density induced by injection molding result in defects during sintering. Critical locations are also the result of two feedstock streams meeting (weld line). [24, 25]

Recently, majority of researchers dealt with the stages of sintering and debinding. These steps are the most unpredictable. There must be a satisfactory removal of binder and uniform shrinkage during sintering. New methods of debinding such as catalytic and super critical partially removed some of these problems.

Understanding the rheological behavior, important for designing both the process and the final product, is currently one of the challenging tasks. In some cases, defective products reach up to 25 % due to nonoptimized molding/flow properties. This is both ecologically and economically unacceptable. [6, 24, 25]

2.2 Rheology of PIM feedstocks

Rheology is the science considering flow deformation of materials under controlled testing conditions. Viscous materials flow by shearing. Imagine two parallel plates separated by a distance (Figure 16). Between the plates there is a liquid (melt) and the bottom plate is fixed. The upper plate moves with the speed induced by shear force F acting on the area A . The resulting shear stress is derived from:

$$\tau = F/A \quad (1)$$

The shear stress causes the flow of PIM feedstock on over a surface. The relative movement of the liquid above the surface is called shear strain γ . When we divide shear strain by the time we get the shear strain rate (shear rate). Proportionality factor between shear stress and shear strain rate is called viscosity of the liquid η . Viscosity is a measure of the resistance of a fluid to the form:

$$\tau = \eta (d\gamma/dt)^n \quad (2)$$

Where n is the exponent used to characterize to fluid. Viscosity of some substances such as water does not depend on shear rate, but only on the temperature and pressure. These fluids are known as Newtonian ($n=1$). PIM materials exhibit more complex behavior. The viscosity of these materials varies with shear rate, but also with temperature and pressure. The most of PIM material are pseudoplastic ($n<1$). A fluid resistance to flow (viscosity) decreases with an increasing shear rate. [5, 22]

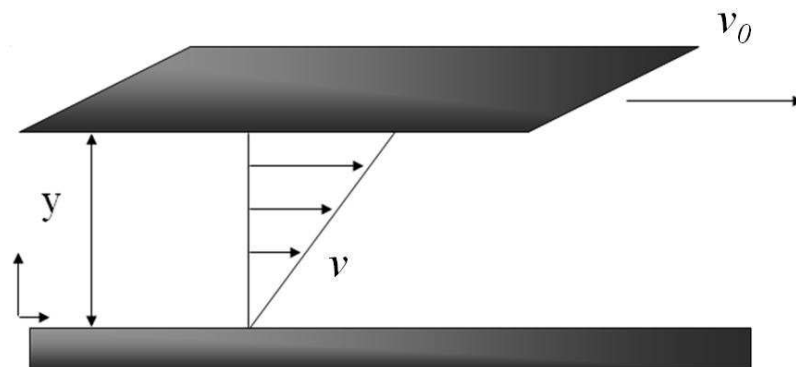


Figure 16 : Basic rheological model [22]

This is only a basic *power-law* model. Most of highly filled systems behave much more complex. Therefore, such simple model must be substituted with more complex ones. Still, these models (Table 3) were originally derived for pure polymer melts.

Table 3: Mathematic models of rheological behaviors

Model	Mathematical description
Herschel-Bulkley	$\tau = \tau_0 + m\dot{\gamma}^n$
Sisko (modified)	$\tau = \tau_0 + \eta_\infty\dot{\gamma} + \eta\dot{\gamma}^n$
Casson	$\tau^{\frac{1}{2}} = \tau_0^{\frac{1}{2}} + (k\dot{\gamma})^{\frac{1}{2}}$
Cross	$\tau = \dot{\gamma} \left[\eta_\infty + \frac{\eta_0 - \eta_\infty}{1 + \lambda\dot{\gamma}^n} \right]$
Carreau	$\tau = \dot{\gamma} \left[\eta_\infty + (\eta_0 - \eta_\infty) \left(1 + (\lambda\dot{\gamma})^2 \right)^{(n-1)/2} \right]$

Explanatory: τ – shear stress, μ – Newtonian viscosity, $\dot{\gamma}$ - shear rate, m – measure of the consistency of the fluid, n – non Newtonian exponent, τ_0 - yield stress, η_1 - second Newtonian plateau viscosity, η - shear viscosity, k – Casson model constant, η_0 - first Newtonian plateau viscosity, λ – relaxation time. [28]

The main factor influencing the phase separation is viscosity and homogeneity of PIM feedstock, but also factors such as air traps, dead zones or weld lines arising from the mold/part design.

Viscosity

Viscosity of a feedstock varies with solid loading. Generally, the higher is the content of the powder, the higher is viscosity (Figure 17).

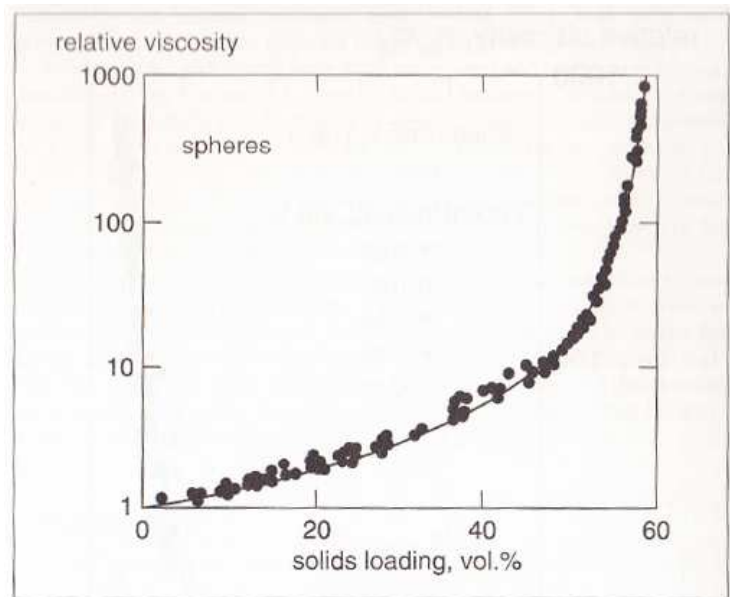


Figure 17: Viscosity dependence on the solids loading [5]

With more powder (less binder) powder particles attain a closer contact. When they are in a full contact, the binder is locked by surrounding particles and becomes immobile, Figure 18. There is no binder to cover particles allowing their movement (flow). In such case viscosity of a PIM feedstock increases beyond all limits. [5]

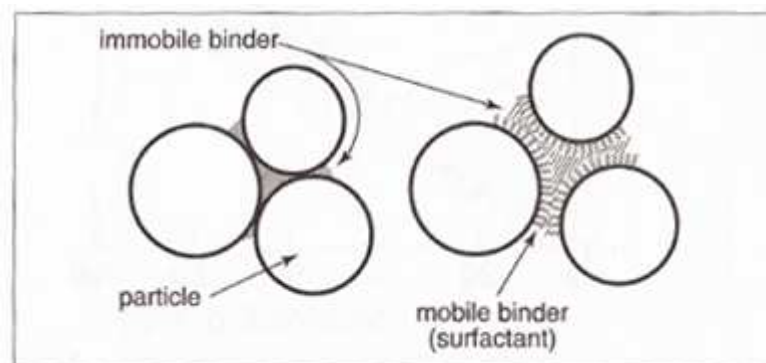


Figure 18: Particles of powder with mobile and immobile binder. [5]

Viscosity is sensitive to temperature. At high temperature binder is less viscous and thus enhancing separation problems during molding. On the other hand, as already mentioned, low temperature causes problems with unacceptable high viscosity of feedstock. [5]

2.3 Homogeneity

Homogeneity of materials can be recognized by the smooth flow curves observed from a capillary rheometer. In the capillary rheometer a material is pushed by the piston through a gap. Capillary rheometer measures the inlet pressure or force applied to the piston and the mass flow. If the pressure or force is independent on the time, it proves the homogeneity of materials. An inhomogeneous material has irregular values. Typical flow curves obtained can be seen in Figure 19. [11]

To measure the homogeneity we can use also a torque rheometer, Figure 20. There are several geometries of torque rheometers such as concentric cylinders, cone and plate or plate and plate. The torque rheometers are rotation devices in which the torque is measured as a function of angular frequency.

To measure the homogeneity of PIM materials capillary rheometers are more suitable since they generate greater shear rates, and thus operate at flow conditions closer to injection molding. On the other hand, torque rheometer can be used to study the mixing process and material structure. [11, 23]

Rheometers are employed not only to study the homogeneity of the feedstock, but also behavior of the feedstock during mixing and its processing properties.

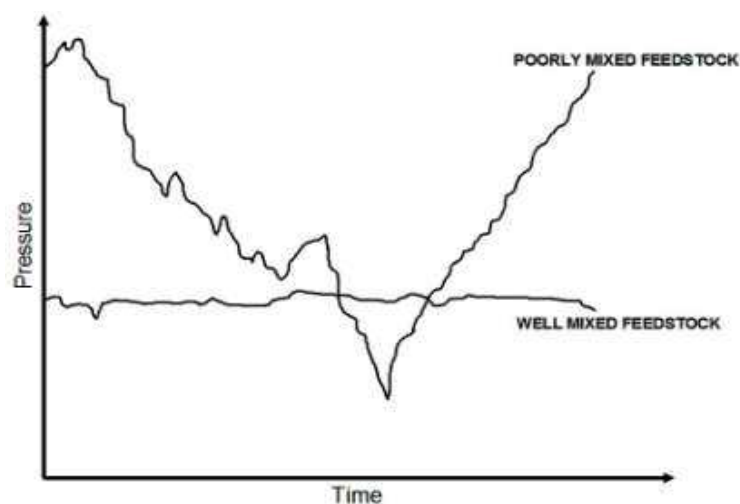


Figure 19: Capillary rheometer – homogenous and inhomogeneous feedstock [11]

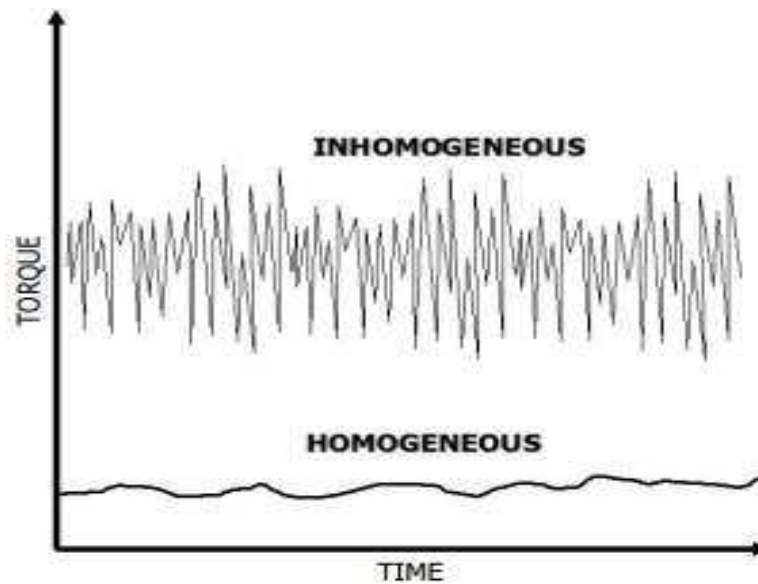


Figure 20: Torque rheometer – homogenous and inhomogeneous feedstock [11]

The most problems occurring during debinding are due to the inhomogeneous feedstock. Debinding makes these problems even more visible. [5]

2.4 Effect of shear rate

A study published by Thornagel [3] deals with the effect of shear rate on the separation. The local shear rate gradient causes the powder to leave these areas with high gradients, and this is the main initiator of phase separation. Near the wall of the channel shear rate attains higher values. On the other hand, in the middle of the channel plateau with a lower value of shear rate is formed (Figure 21). Due to this non-uniform shear rate, there is a rotation of particles near the wall. It is expected that the rotating particles try to get to an area with lower shear rate. The result is an area near the wall, showing a high concentration of separated binder, while the powder particles are grouped in the middle of the channel with the lower value of shear rate. [3]

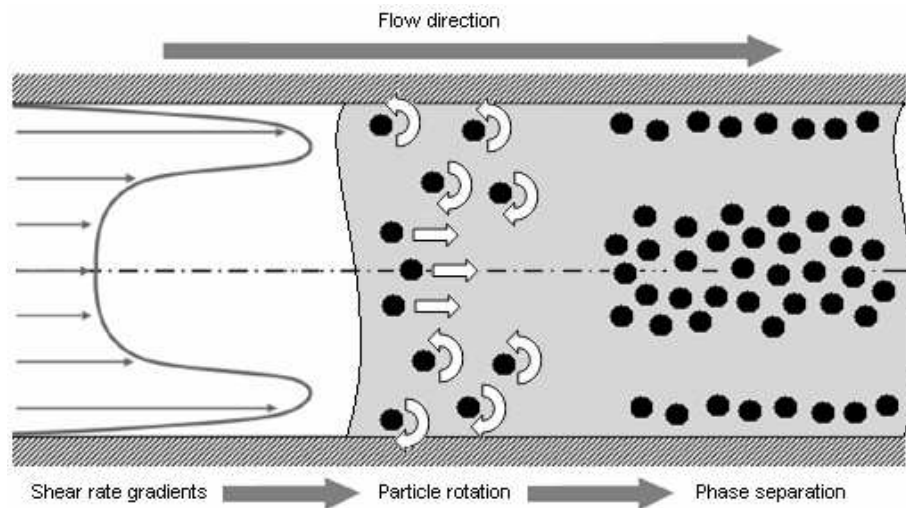


Figure 21: Phase separation - effect of shear rate gradient [3]

2.5 Moldability

Moldability combines conditions under which the component is formed. These conditions are temperature and pressure. The complexity of this process can be seen in the graphical representation. Schematic Figure 22 shows entire molding process. Left part of the diagram shows course of screw speed to fill a mold. Mold filling rate must be precisely controlled. Poor process control leads to the creation of defects. The right part of the diagram shows pressure profile. The course of pressure must be controlled precisely too.

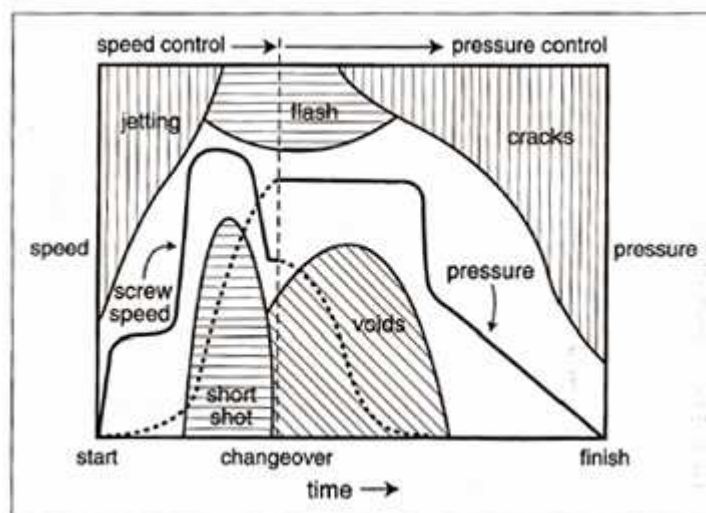


Figure 22: Schematic diagram of defects during entire molding process [5]

Relations among defects, combinations of feedstock temperature and share rate are summarized in Figure 23. [5]

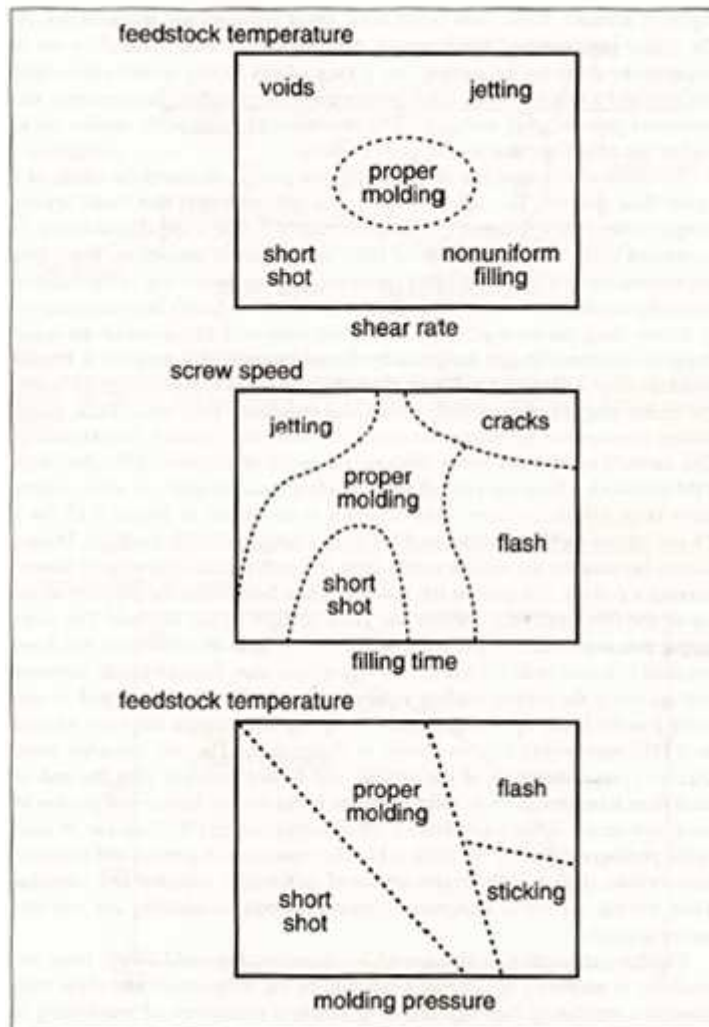


Figure 23: Molding defects [5]

Moldability and the associated phase separation are usually tested on a thin spiral mold. Precisely defined spiral (165 cm long, 3 mm deep and 4.8 mm wide) is filled with a feedstock. Moldability is determined by the length of the filled spiral. Because the wall of spiral is cold, a continuous frozen layer is formed along this wall. Gradually, the channel is closed and the flow stops. The effect is called a fountain flow, and it is illustrated in Figure 24. [5, 27]

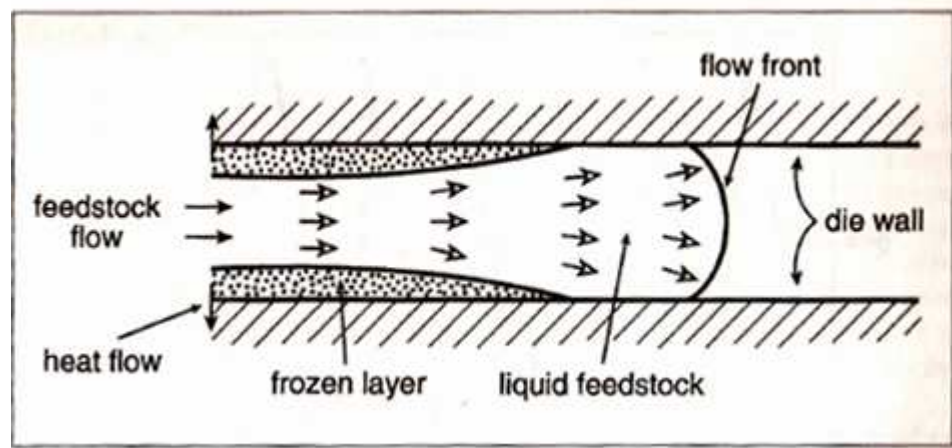


Figure 24: Origin of a fountain flow [5]

Filled length of the spiral and moldability are higher for low viscosity/low solid loading.

The shape of the testing molds can be also square spiral or zig-zag as shown in Figure 25.

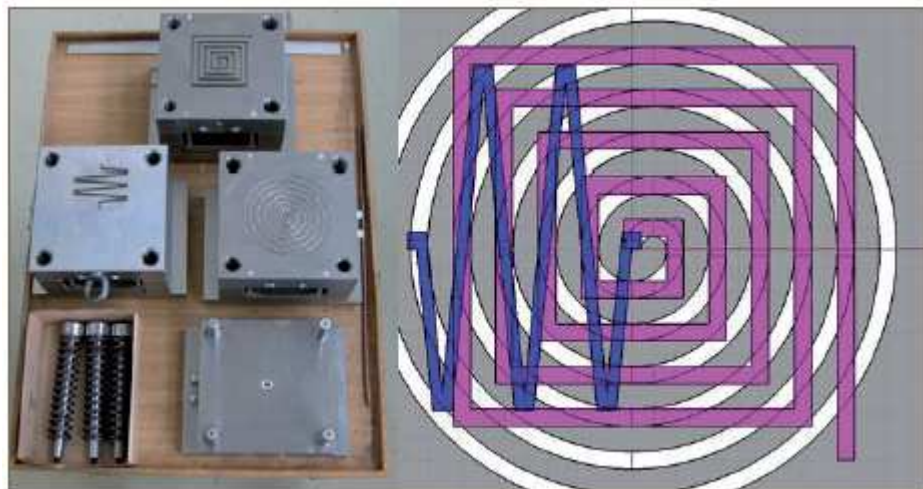


Figure 25: Moldability testing molds [27]

Separation study employing various testing molds was published by Jenni et al. [27]. Simulation software was used to compare the experimental sample with a balance model. The balance model represents the flow of solid, spherical particles in a Newtonian fluid. The behavior of samples during mold filling was monitored with differential scanning calorimeter (DSC).

Experiment was performed under various conditions. The main variables were nozzle temperatures, mould temperature and injection speed. Moldability was found to be strongly dependent on these factors. Varying these parameters optimal conditions were derived. It was found that better fluidity is achieved with higher temperature and injection speed.

Further, the flow length depends on the solid loading. Comparing 60 vol. % and 50 vol. % solid loadings, the difference of the filled length attained was about 68 %.

A fountain flow effect is also enhanced with temperature and injection speed. This is due to a lower viscosity of binder. The binder flow more easily and the particles of powder remain behind. Lowering temperature and injection speed reduce phase separation. [27]

Finally, experimental results were compared with balance model. Simulation software produced two and three dimensional pictures of the powder distribution. Phase separation was located mostly in the corners. Samples were prepared by horizontal cutting a corner in the three parts with 1 mm height out from the middle. Thus, the prepared corner was cut into 64 sections with a thickness of 1 mm. Measurements were performed using radiography, computer tomography and DSC. The results were not adequate, because tungsten has high density as well as absorption. Another disadvantage of this method is low resolution of pictures. The method also does not account for wall effects like slip, rolling of particles and layer with an excess of binder. [27]

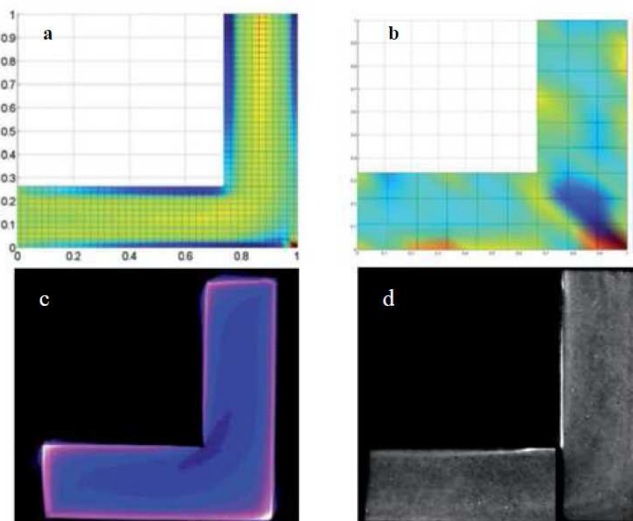


Figure 26 : 2D distribution of the powder in the corner of the square spiral mold.

a - balance model, b - DSC, c - tomography, d - radiography [6]

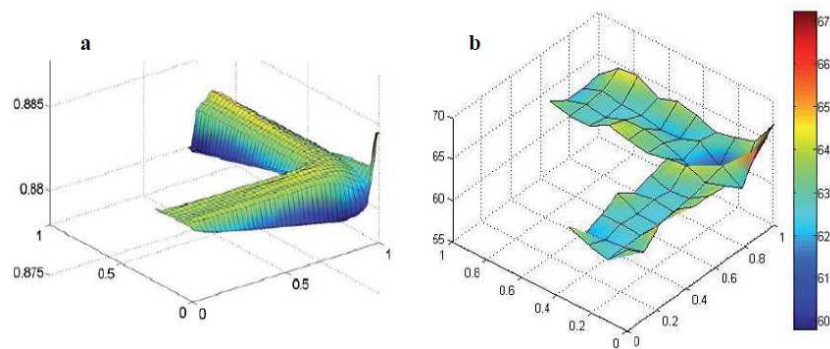


Figure 27 : 3D distribution of the powder in the corner of the square spiral mold.
a - balance model, b - DSC [6]

2.6 Design of a mold testing powder and binder separation

Mold developed at the Polymer Centre, TBU in Zlín [6] (in cooperation with Fraunhofer IFAM, Bremen) was designed to test the phase separation. This mold contains the critical elements as:

- Inner and outer corners
- Radical thickness changes including gates
- Weld lines
- Thin films and flashes

Design of the testing mold is shown in Figure 28.

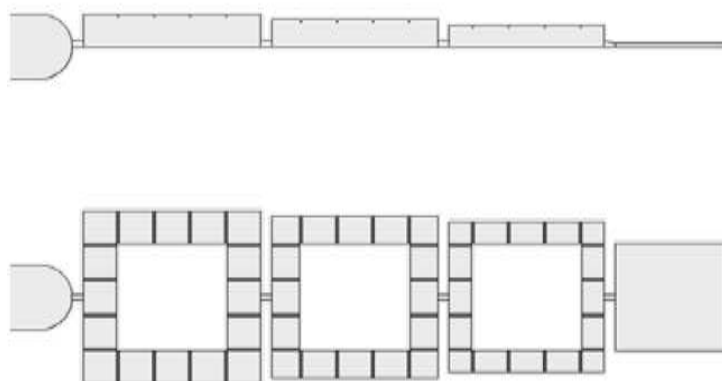


Figure 28: Testing mold [3]

The testing mold is composed of four elements connected by gates. The first three elements contain the external and internal corners. These elements are used to study the development of the phase separation within the flow. Fourth element plagues as drainage area for the third element. Size of the inner wall of the first three elements is 10 mm. Length of the sides of square cross section is then gradually decreased from 3 mm to 2.5 mm and 2 mm. Each element contains 16 slots for better orientation. Flat element is 0.3 mm high. Gates between the elements are 1 mm long and 0.5 mm wide. [6]

The most visible separation is around the gate to each element as can be seen from Figure 29. [6]

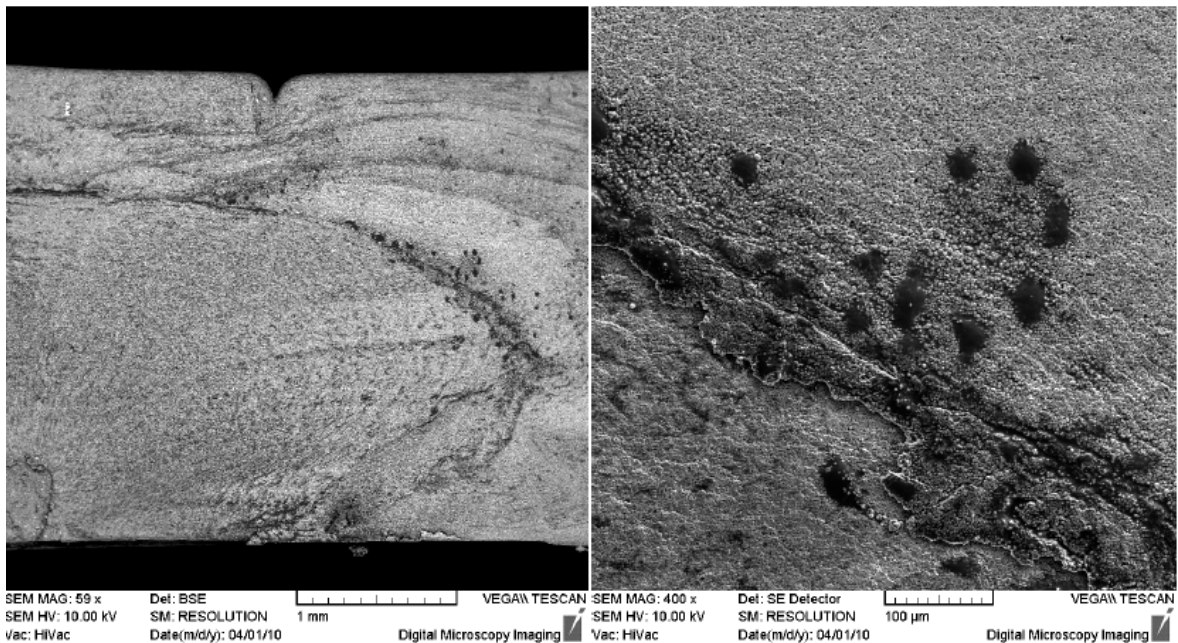


Figure 29 : SEM of phase separation [6]

A more complicated problem arises when quantitative evaluation of separation is needed. This problem is the main aim of the practical part this master thesis.

II. ANALYSIS

3 AIM OF THE MASTER THESIS

The aims of the experimental part are:

- Optimization of injection molding process for two feedstocks
- SEM microscopy
- Energy dispersive X-ray spectroscopy
- Characterization of materials
- Quantitative evaluation of the separation

To study the phase separation the testing mold described in the theory section 2.6 was employed.

4 OPTIMIZATION OF INJECTION MOLDING PROCESS

4.1 Injection molding machine

Process optimization was performed on the injection molding machine Arburg Allrounder 370S (EUROMAP size 700-100).



Figure 30: Arburg Allrounder 370S

Table 4: Technical data for Arburg Allrounder 370S

Clamping unit		Injection unit	
Clamping force (max.)	700 kN	Screw diameter	30 mm
Closing force (max.)	38 kN	Effective screw length	16.7 L/D
Opening force (max.)	160 kN	Screw stroke (max.)	100 mm
Opening stroke (max.)	400 mm	Calculated injection volume (max.)	71 cm ³
Mould height (min.)	200 mm	Shot weight (max.)	65 g PS
Daylight (max.)	600 mm	Injection pressure (max.)	2500 bar
Distance between tie bars	370 x 370 mm	Injection flow (max.)	204 cm ³ /s
Platen size	510 x 510 mm	Peripheral screw speed (max.)	59 m/min
Weight of movable mold half (max)	360 kg	Screw torque (max.)	180 Nm
Ejector force (max.)	30 kN	Back pressure positive/ negative (max.)	350 / 200 bar
Ejector stroke (max.)	125 mm	Material hopper capacity	50 l

4.2 Feedstock

Two commercially available stainless steel feedstocks were used: polyMIM[®] 316L supplied by Polymer-Chemie, GmbH, and Catamold[®] 316L developed by BASF, GmbH. According to the data sheets (summarized in Tables 5 and 6) and performance, these materials are similar in terms of powder characteristics.

Table 5: Properties of PolyMIM[®] 316L

Product	PolyMIM [®] 316L								
Product description	Feedstock for Metal Injection Molding								
Oversize factor	min-			average			max.		
	1.1627			1.1669			1.1711		
MVR melt index	min.			average			max.		
	15			40			65		
Typical composition (as sintered in weight%)	Fe	C	Ni	Cr	Mo	Mn	Si	S	P
	Balance	<0.03	10.0- 14.0	16.0-18.5	2.0-3.0	<2.0	<1.0	<0.03	<0.045
Typical properties	As sintered								
	Density			≥7.90 g/cm ³					
	Yield strength			≥140 MPa					
	Tensile strength			≥450 MPa					
	Elongation			≥40 %					
	Hardness			≥150 HV1					
Injection molding process	Cylinder temperature				Zone1	Zone2	Zone3	Zone4	Nozzle
					170°C	175°C	180°C	183°C	185°C
	Tool temperature				40-60 °C				
	Injection speed				3-20 cm ³ /s				
	Screw circumferential speed				5-20 m/min				
	Injection pressure				550-700 bar				
	Post pressure				400-650 bar				
	Back pressure				20-30 bar				
Debinding process	Solvent				Water				
	Debinding temperature				40-60 °C				
	Debinding time				Depending on part thickness (e.g. 4 mm part, approx. 10 h at 60 °C)				
	Weight loss				>3.8 weight %				
	Drying				to constant weight (approx. 2 h, 100 °C)				
Sintering process	Sintering atmosphere				100 % pure hydrogen				
	Sintering cycle				3 K/min → 600 °C, 2 h hold 600 °C, 5 K/min → 1320 °C, 2 h hold 1320 °C, 15 K/min → 80 °C, cooling				

Table 6: Properties of Catamold[®] 316L

Product	Catamold [®] 316L						
Product description	Feedstock for Metal Injection Molding						
Oversize factor	min.		average			max.	
	1.1629		1.1669			1.1710	
MVR melt index	min.		average			max.	
	350		450			700	
Typical composition (as sintered in weight %)	Fe	C	Cr	Ni	Mo	Mn	Si
	Balance	<0.03	16-18	10.14	2.3	<2	<1
Typical properties	Density		≥7.90 g/cm ³				
	Yield strength		≥180 MPa				
	Tensile strength		≥510 MPa				
	Elongation		≥50 %				
	Hardness		≥120 HV1				
Injection molding process	Cylinder temperature		Zone1	Zone2	Zone3	Zone4	Nozzle
			150°C	160°C	170°C	180°C	190°C
	Tool temperature		128 °C				
	Injection speed		10 cm ³ /s				
	Screw circumferential speed		50 min ⁻¹				
	Injection pressure		900 bar				
	Post pressure		90 bar				
	Back pressure		0 bar				
Debinding process	Solvent		HNO ₃ > 98 %				
	Debinding temperature		110 °C				
	Debinding time		Depending on part thickness				
	Weight loss		>7.6 weight %				
	Drying		to constant weight				
Sintering process	Sintering atmosphere		100 % pure hydrogen				
	Sintering cycle		5 K/min → 600 °C, 1 h hold 600 °C, 5 K/min → 1380 °C, 3 h hold 1320 °C, cooling				

4.3 Injection molding process

In the first step, the molding parameters from the data sheet were set up, but it resulted in an incomplete filling of the mold (short shot), Figure 31a. Therefore, the pressure and hold pressure were gradually increased, while keeping injection and screw speeds. When the pressure reached 2,000 bar, the testing mold was still not completely filled. Further

increasing the pressure did not bring better filling. Thus, temperatures were increased in all zones and on the nozzle, which was considered as optimum. Additionally, the optimum cooling time was set at 30 s. The ejecting apparatus damages the sample if cooling time was lower. Optimally injected sample is depicted in Figure 31b.

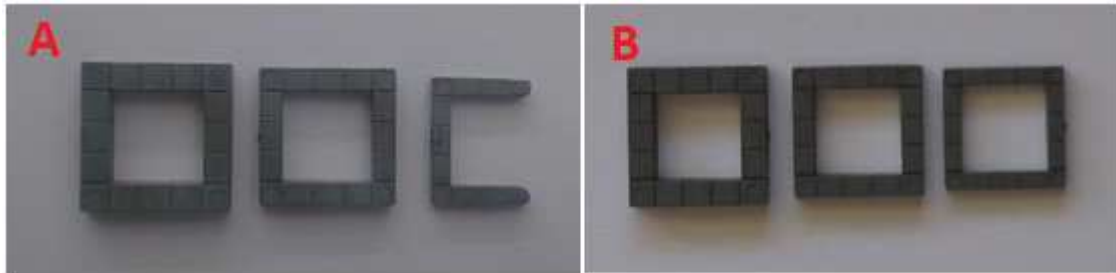


Figure 31: Injection molded testing samples: a - short shot, b - optimized.

The optimized molding conditions for polyMIM[®] 316L and Catamold[®] 316L are summarized in Table 7.

Table 7: Optimized molding conditions

Material	PolyMIM [®] 316L	Catamold [®] 316L
Zone 1 temperature (°C)	160	160
Zone 2 temperature (°C)	185	170
Zone 3 temperature (°C)	190	180
Zone 4 temperature (°C)	195	190
Nozzle temperature (°C)	200	200
Mold temperature (°C)	85	85
Injection speed (mm/s)	220	188
Injection pressure (bar)	2000	2000
Injection time (s)	0.19	0.19
Hold pressure (bar)	2100	2100
Hold pressure time (s)	4.0	4.0

5 SCANNING ELECTRON MICROSCOPY

Similarly to optical microscope, electron microscope is an optical instrument in which photons are replaced by electrons and glass lenses are replaced by electromagnetic ones. Due to the shorter wavelength of electrons the resolution of the electron microscope is much greater (up to thousand times) than that of the optical. The first type of electron microscope was transmission electron microscope (TEM) developed by Ruska in 1931. Later type is scanning electron microscope (SEM). This type was constructed by Zworykin in 1942. Samples analyzed with electron microscopy must be conductive, therefore nonconductive materials must be metal plated before testing.

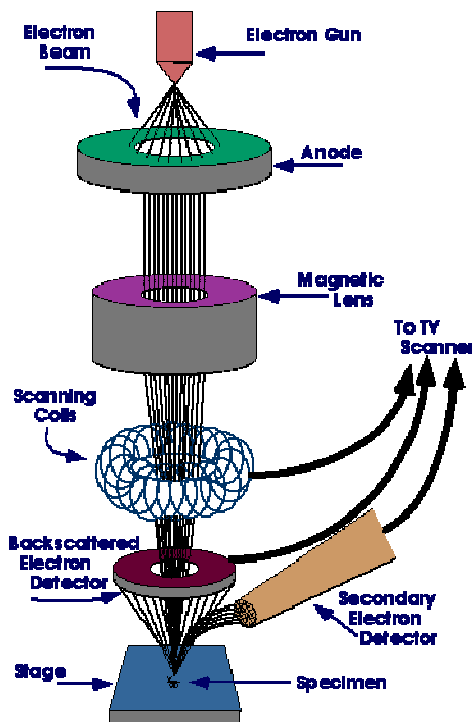


Figure 32: Scheme of scanning electron microscope

Principle of SEM is shown in Figure 32. Electrons are accelerated by the anode. The magnetic field directs and focuses the electron beam. The focused electron beam then strikes the sample. Two types of electrons can be detected - secondary electron (SE) and backscattered electron (BSE).

5.1 SEM analysis of feedstocks

Images were made on four samples for two commercial feedstocks - polyMIM[®] 316L and Catamold[®] 316L. Separation of the main material components (powder and binder) during injection molding was examined. For a complete analysis, unmolded samples were also examined.

Unmolded samples

Unmolded samples were prepared by pressing on a laboratory press machine from the pellets provided by manufactures. Pressing conditions were:

- 2 minutes preheating at 200 °C,
- 3 minutes pressing at 200 °C,
- 5 minutes cooling.

The SEM images were taken at a magnification of 100x and accelerating voltage of 30 kV with BSE detector. The sample scans of unmolded Catamold[®] 316 and PolyMIM[®] 316 can be seen on Figure 33 and Figure 34, respectively.

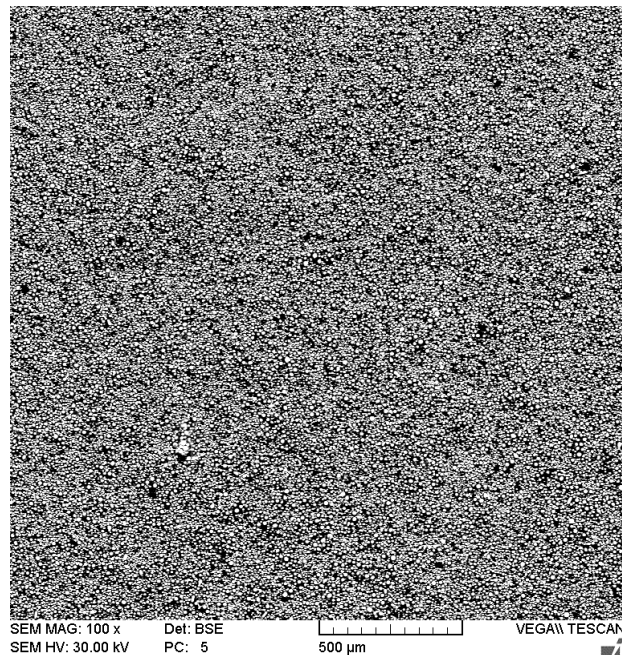


Figure 33: SEM of unmolded Catamold[®] 316 feedstock

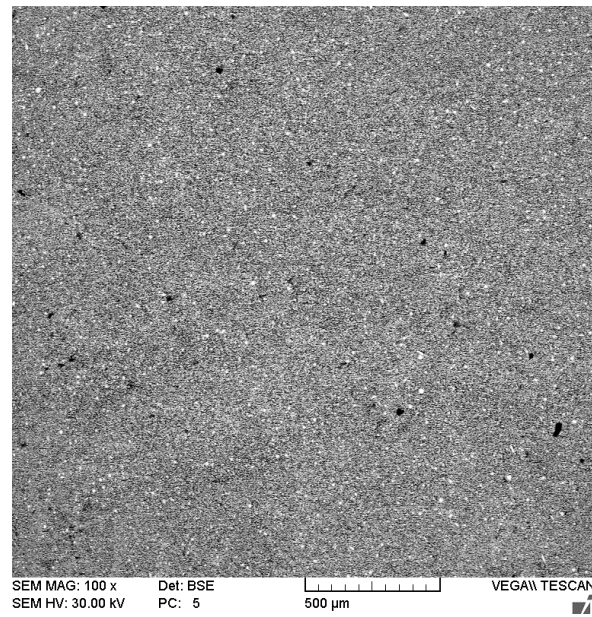


Figure 34: SEM of unmolded PolyMIM[®] 316 feedstock

The images show homogeneous distribution of powder (bright points) and binder (dark points). From the visual observation it seems that Catamold[®] 316 contains more dark places, i.e. has a lower content of powder, than PolyMIM[®] 316. Therefore, more detailed analysis has to be performed.

The lower iron content was confirmed with thermogravimetical (TG) analysis, Figures 35 and 36. The lower powder content of Catamold[®] 316 will result in a different behavior during debinding and sintering.

The different powder:binder ratio is apparent from the TG analysis. Catamold[®] 316 weight loss was 8 %, binder degradation started at 227 °C (Figure 35). PolyMIM[®] 316 weight loss was only 3.8 %. The first weight loss occurred at 170 °C. Besides, a powder oxidation was detected for this feedstock exceeding binder loss around 300 °C (Figure 36).

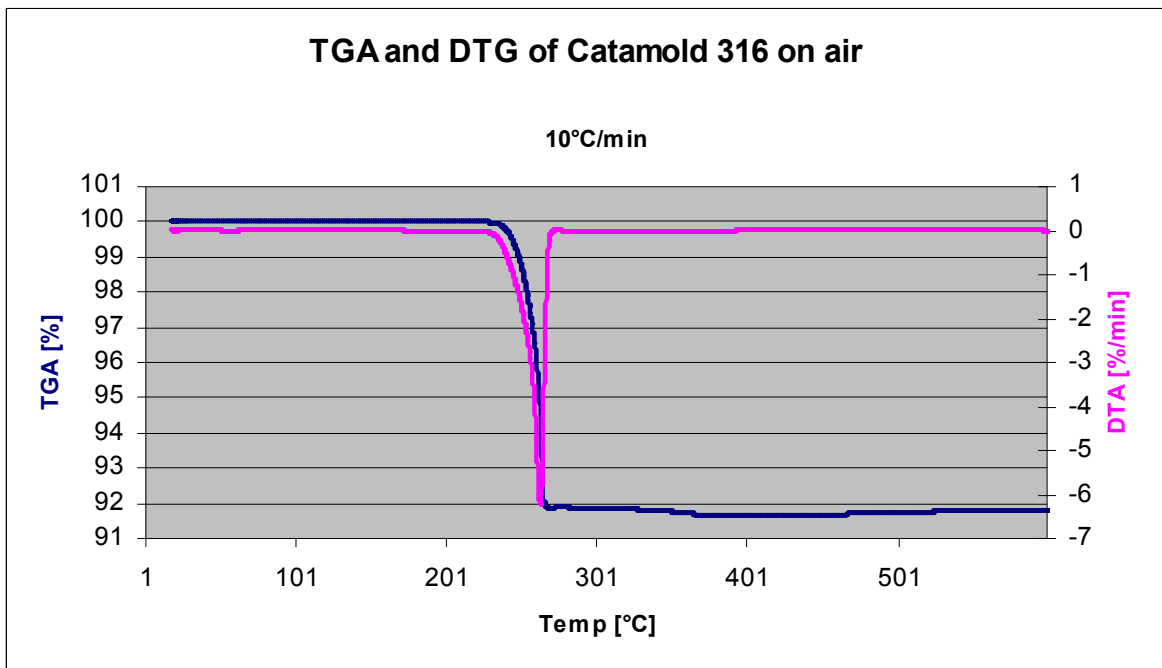


Figure 35: TGA of Catamold[®] 316 on air

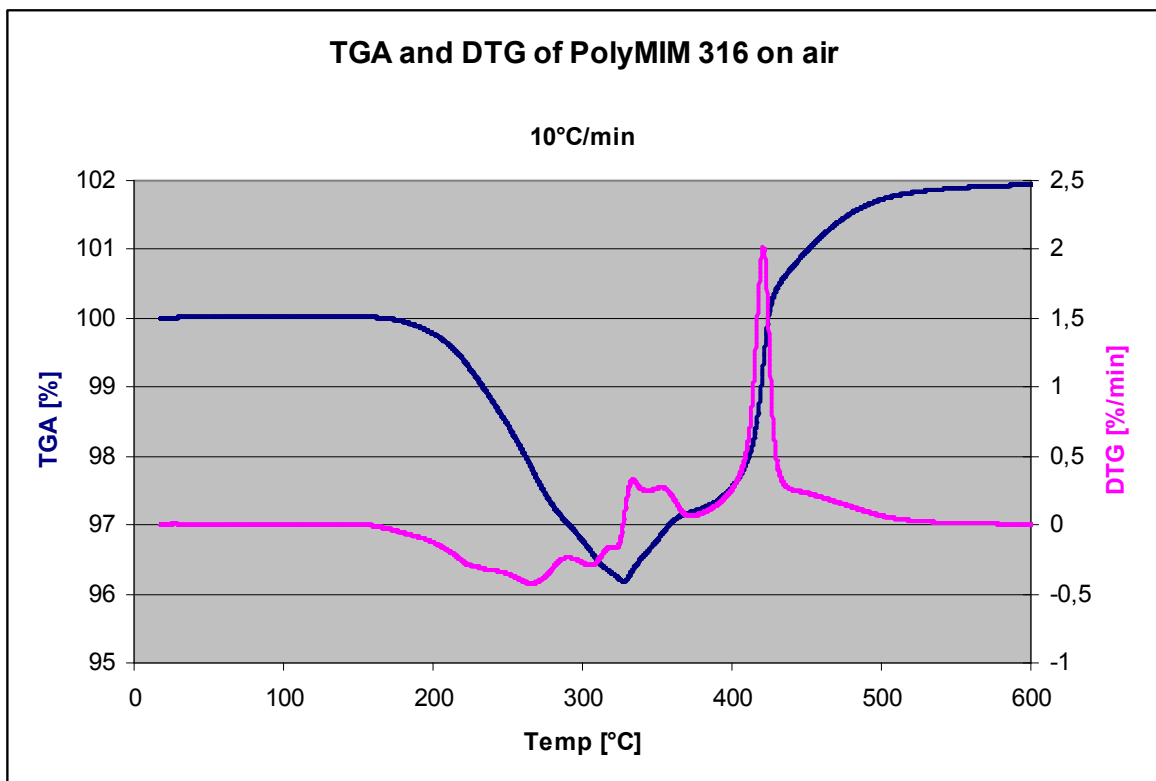


Figure 36: TGA of PolyMIM[®] 316 on air

Samples separated during injection molding

Samples were molded under the conditions described in chapter 4.3. The largest phase separation was detected at the entrance gate to each square element. Therefore, these places were thoroughly investigated by SEM. The precise locations are shown in Figure 37.

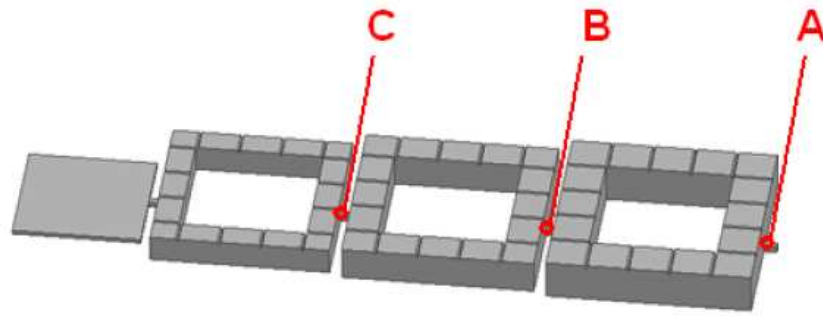


Figure 37: Locations scanned with SEM [6]

The results of SEM analysis are displayed on next Figures. Resolutions 78x, 94x and 115x were used according to the size of the particular square element (A, B, C).

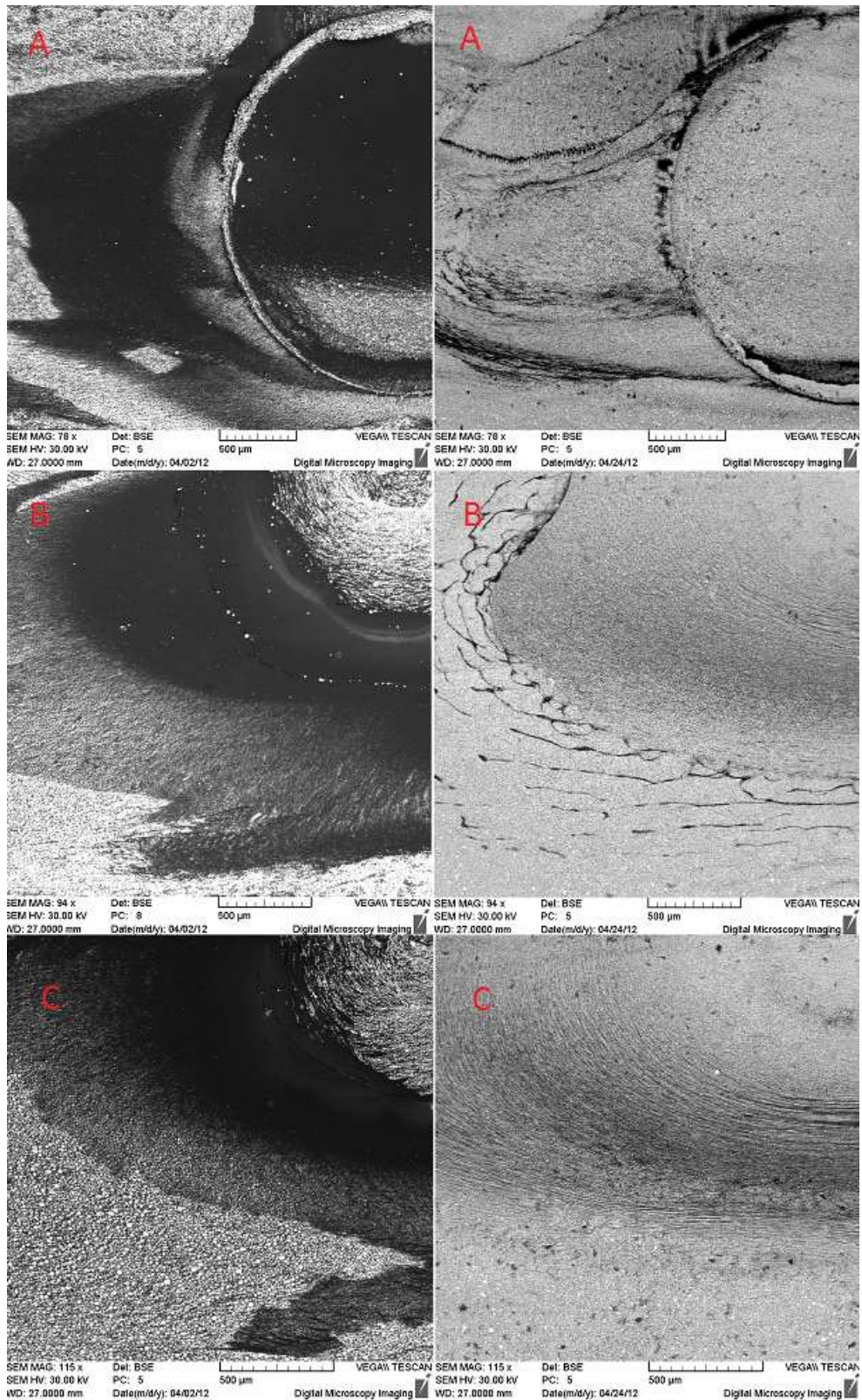


Figure 38: Phase separation located at the gates to the particular testing mold elements.

Left images - Catamold® 316 Right images - PolyMIM® 316

The discrepancies between the separation causes of the two materials tested are clearly visible. Catamold[®] 316 undergoes a larger phase separation. It seems that the phase separation is largest in the area A and less pronounced in the area C. This phenomenon will be investigated in more detail in the following. PolyMIM[®] 316 seems to show smaller phase separation, and it seems less dependent of the position on the sample. It also appears that there is a reduction of phase separation from A to B. Energy dispersive X-ray spectroscopy and following quantitative analysis will respond more precisely to the issue.

5.2 Energy dispersive X-ray spectroscopy

Energy dispersive X-ray spectroscopy (EDX) is an analytical technique used for the elemental analysis or chemical characterization of a sample. All samples were mapped across the gateway area. For the study of phase separation carbon and iron elements were selected. Carbon is the key element in polymer binder and iron is the typical representative element of powder. According to the data sheets, other powder elements are represented only in small quantities, and thus their evaluation would not be representative. Data collection for EDX is 1,800 seconds. It is corresponding to the state, where each point is scanned around 50times. For a better idea of representation of all elements in the sample, the sum spectra were created. Homogeneous and separated samples were mapped. Further, EDX maps will be quantified and degree of separation determined.

5.2.1 EDX mapping

The following Figure 39 and Figure 40 show the sum spectra and EXD maps of unmolded samples of Catamold[®] 316.

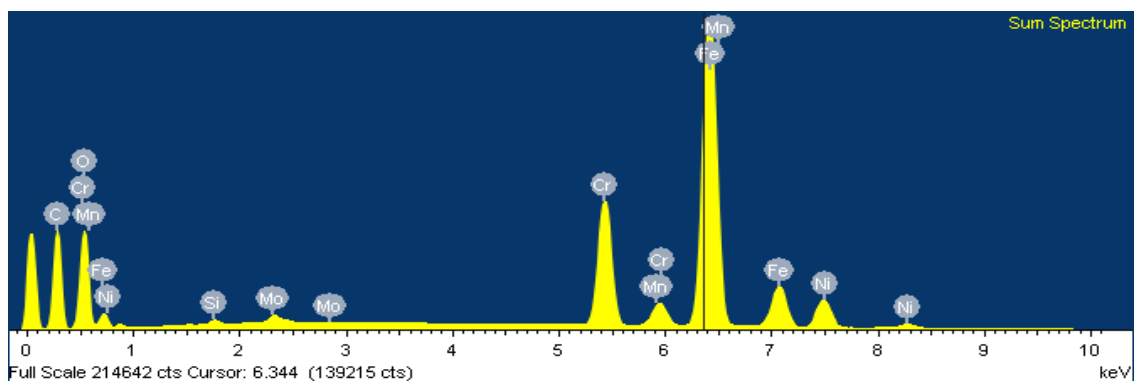


Figure 39: Sum spectrum of Catamold[®] 316

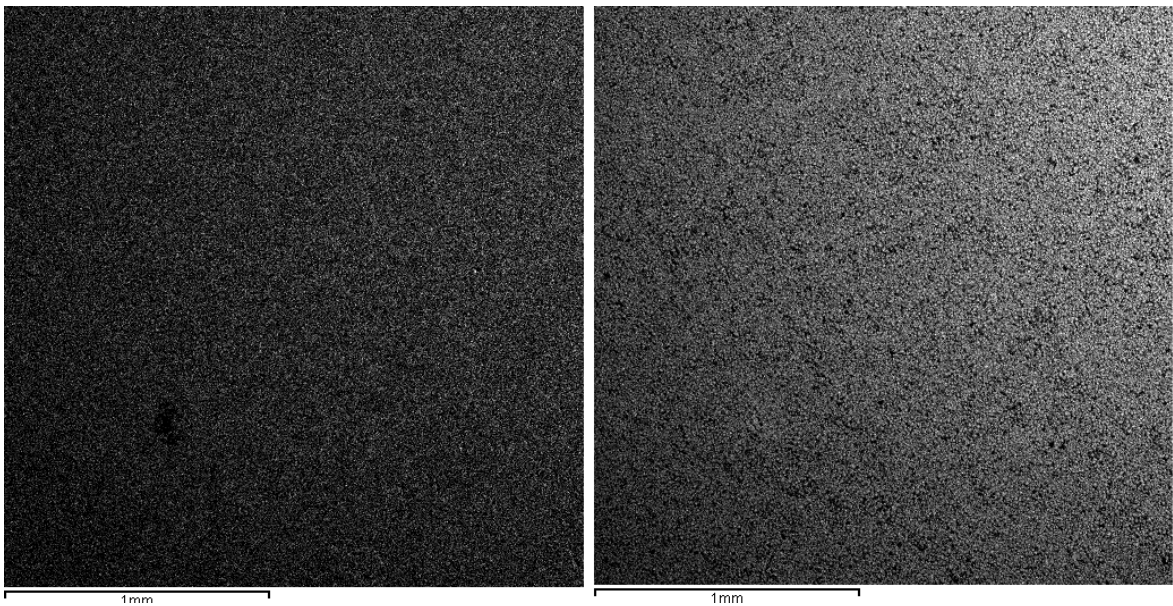


Figure 40: EDX of Catamold[®] 316

Left – Carbon Right-Iron

The contents of all elements were examined using the sum spectrum. In comparison to data sheet (Table 6), the peak corresponding to manganese is unexpectedly high. EDX maps showed homogeneity of feedstock and balanced representation of powder-binder distribution.

The same analysis was provided for testing PolyMIM[®] 316. Results can be seen in the following pictures (Figures 41 and 42).

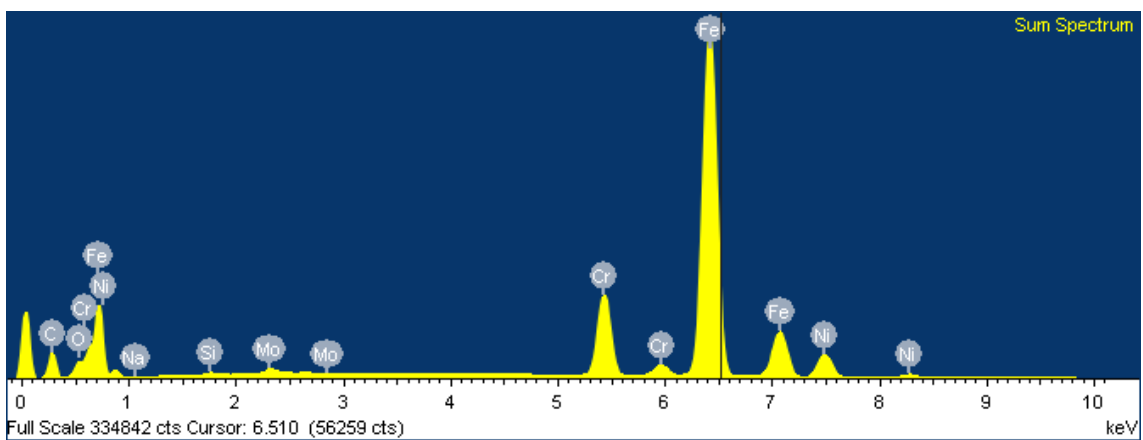


Figure 41: Sum spectrum of PolyMIM[®] 316

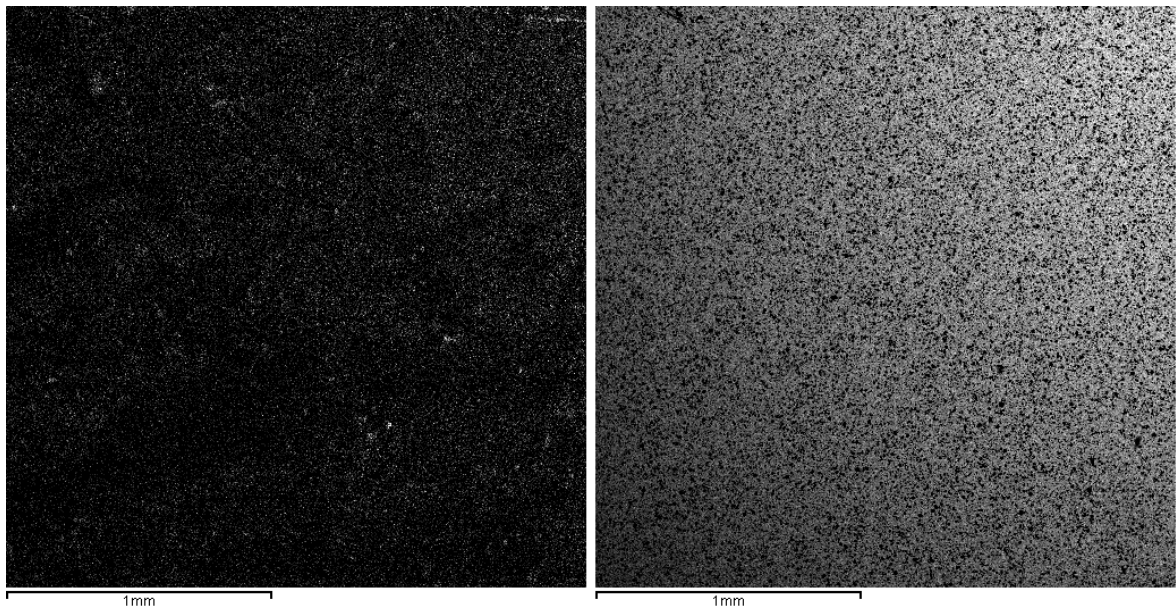


Figure 42: EDX of PolyMIM[®] 316

Left – Carbon

Right – Iron

Homogeneity and content of all elements was confirmed. The highest peak was observed for iron as expected from the data sheet of this feedstock summarized in Table 5.

Separated samples were evaluated in the same way. Results of analysis are shown below. The first group of sum spectra relates Catamold[®] 316, and the second shows PolyMIM[®] 316. The square elements are again marked A, B, C (A - the largest element and C - the smallest element).

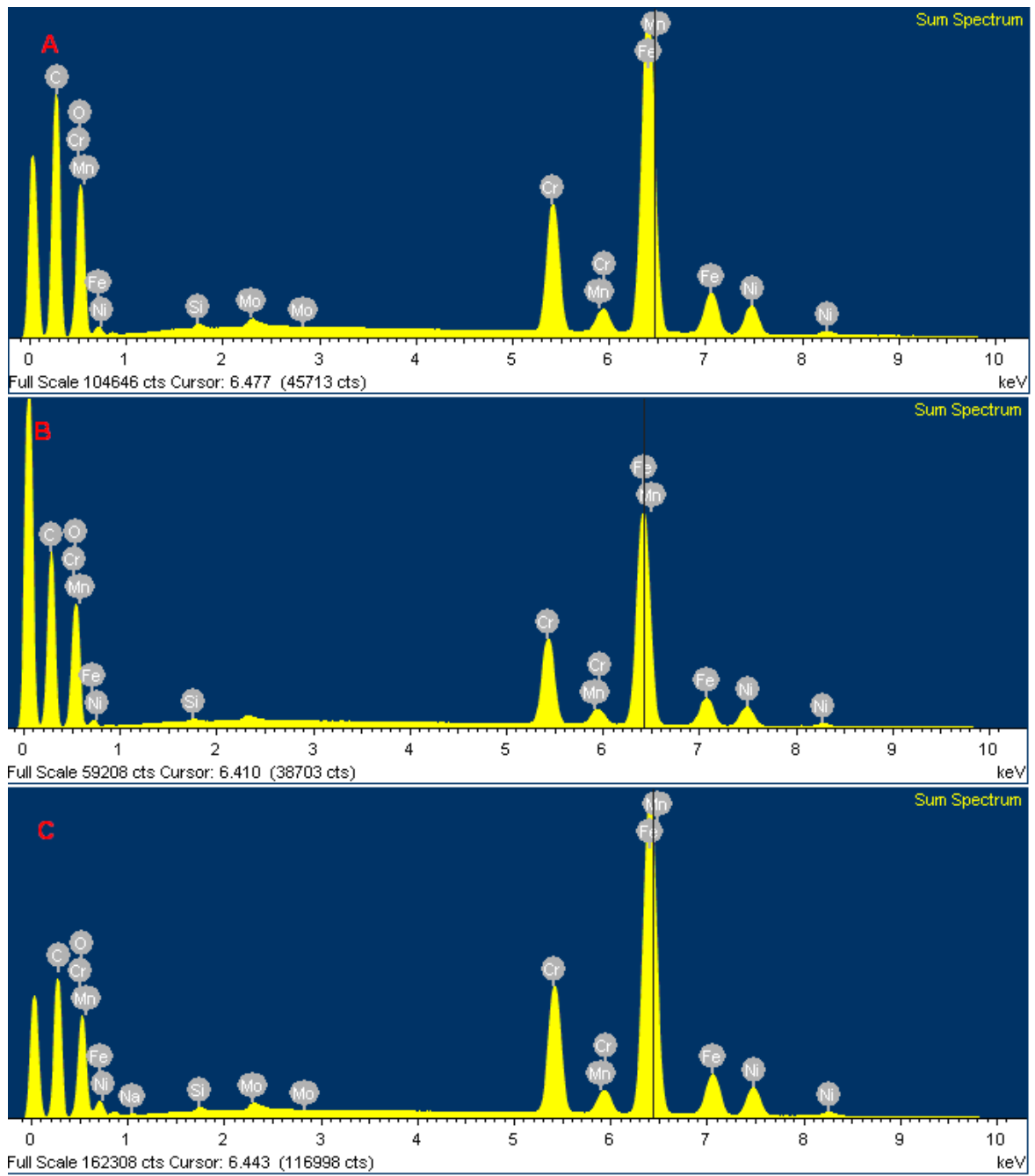


Figure 43: Sum spectra of separated samples of Catamold[®] 316

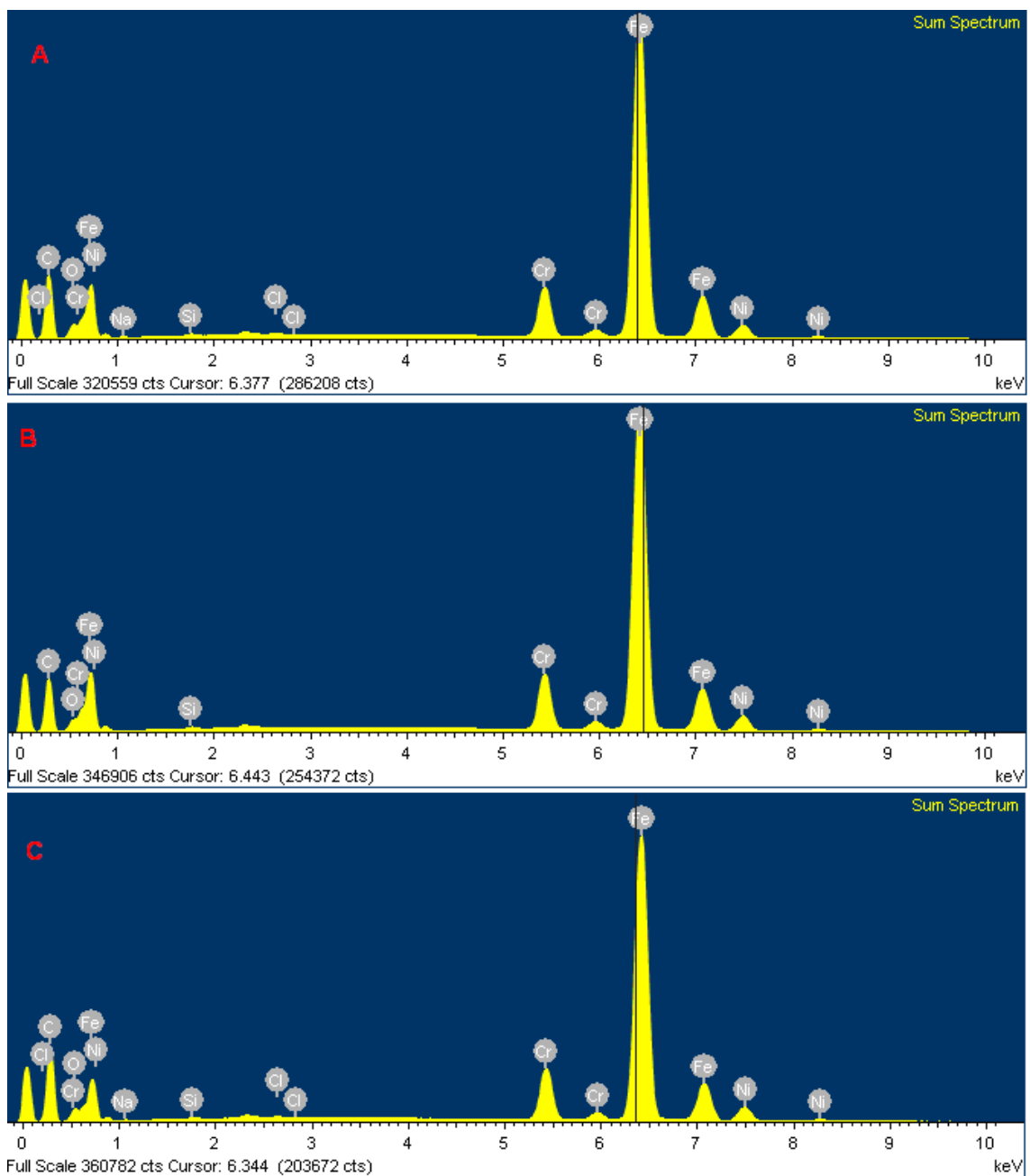


Figure 44: Sum spectra of separated samples of PolyMIM[®] 316

When comparing the spectra, higher iron content in the PolyMIM[®] 316 is obvious.

EDX maps of separated samples are shown below. EDX of iron also confirmed a higher content of iron in PolyMIM[®] 316. Susceptibility of Catamold[®] 316 on the phase separation is also rather evident. PolyMIM[®] 316 has a better homogeneity/lower separation. Development of phase separation from the position at square element A to square element C is not too obvious.

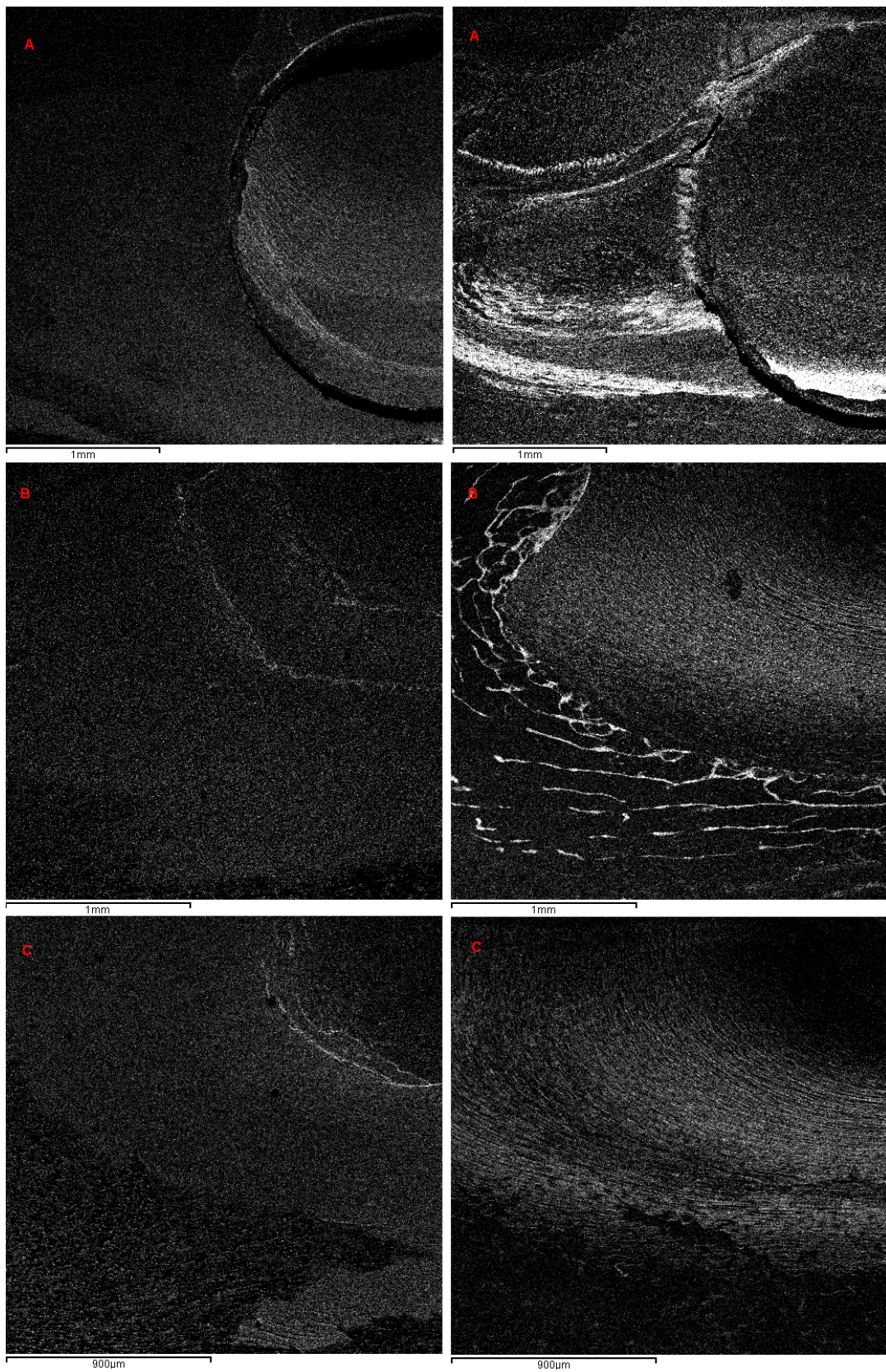


Figure 45: EDX of carbon.

Left images - Catamold® 316 Right images - PolyMIM® 316

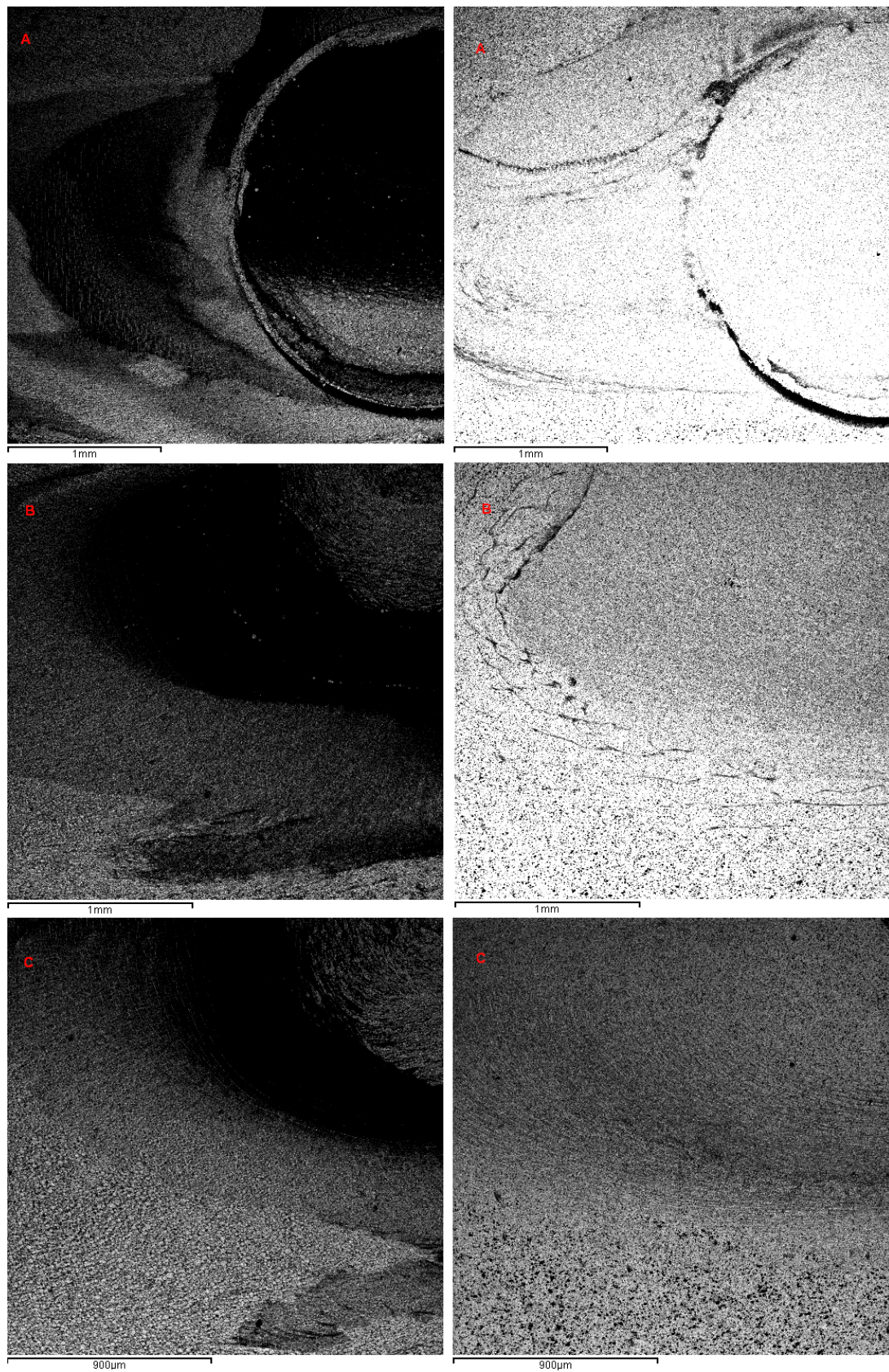


Figure 46: EDX of iron.

Left images - Catamold® 316 Right images - PolyMIM® 316

5.2.2 Quantitative X-ray Mapping

Quantitative X-ray mapping was created. Representation of the elements was calculated at each point. Maps were made with a resolution 128x128. Representation of elements is expressed as weight %.

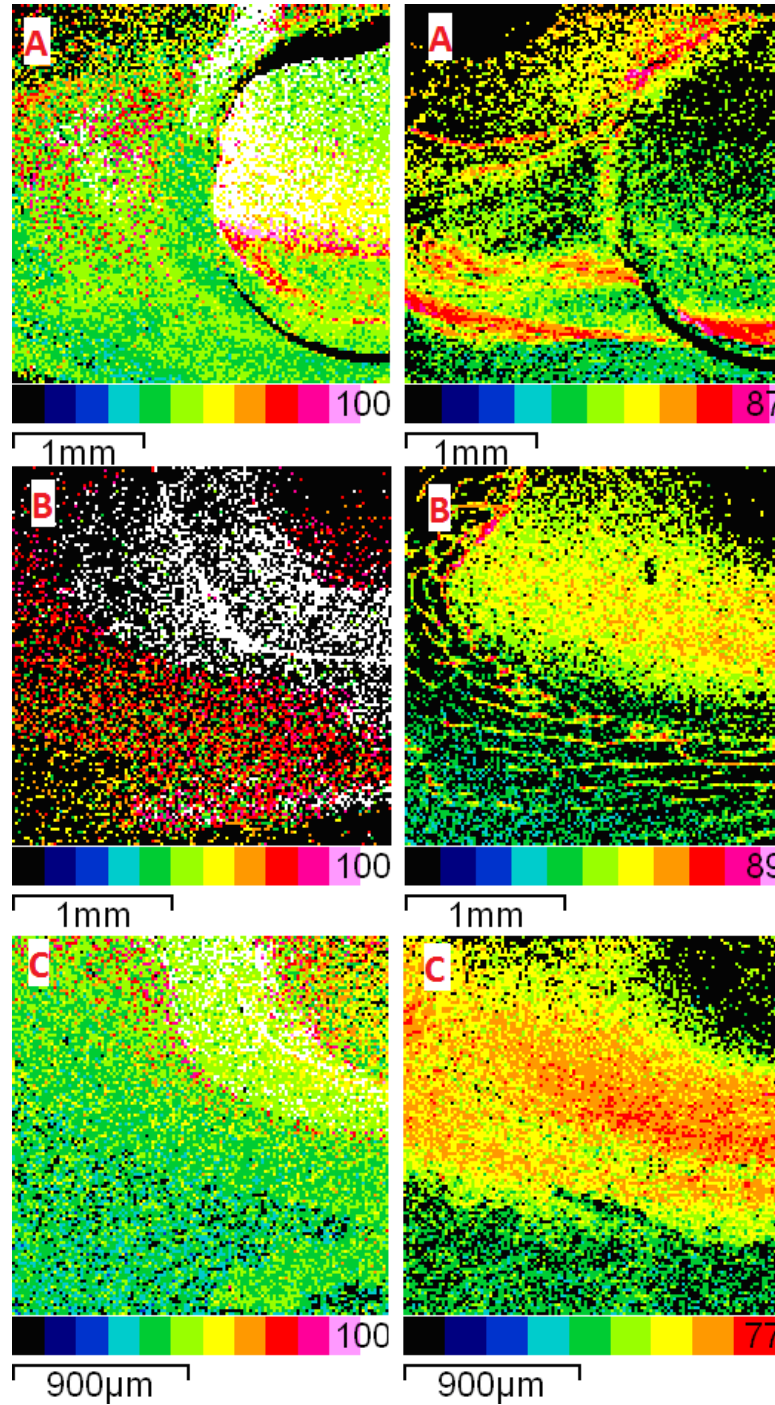


Figure 47: Quantitative X-ray of carbon

Left images - Catamold[®] 316 Right images - PolyMIM[®] 316

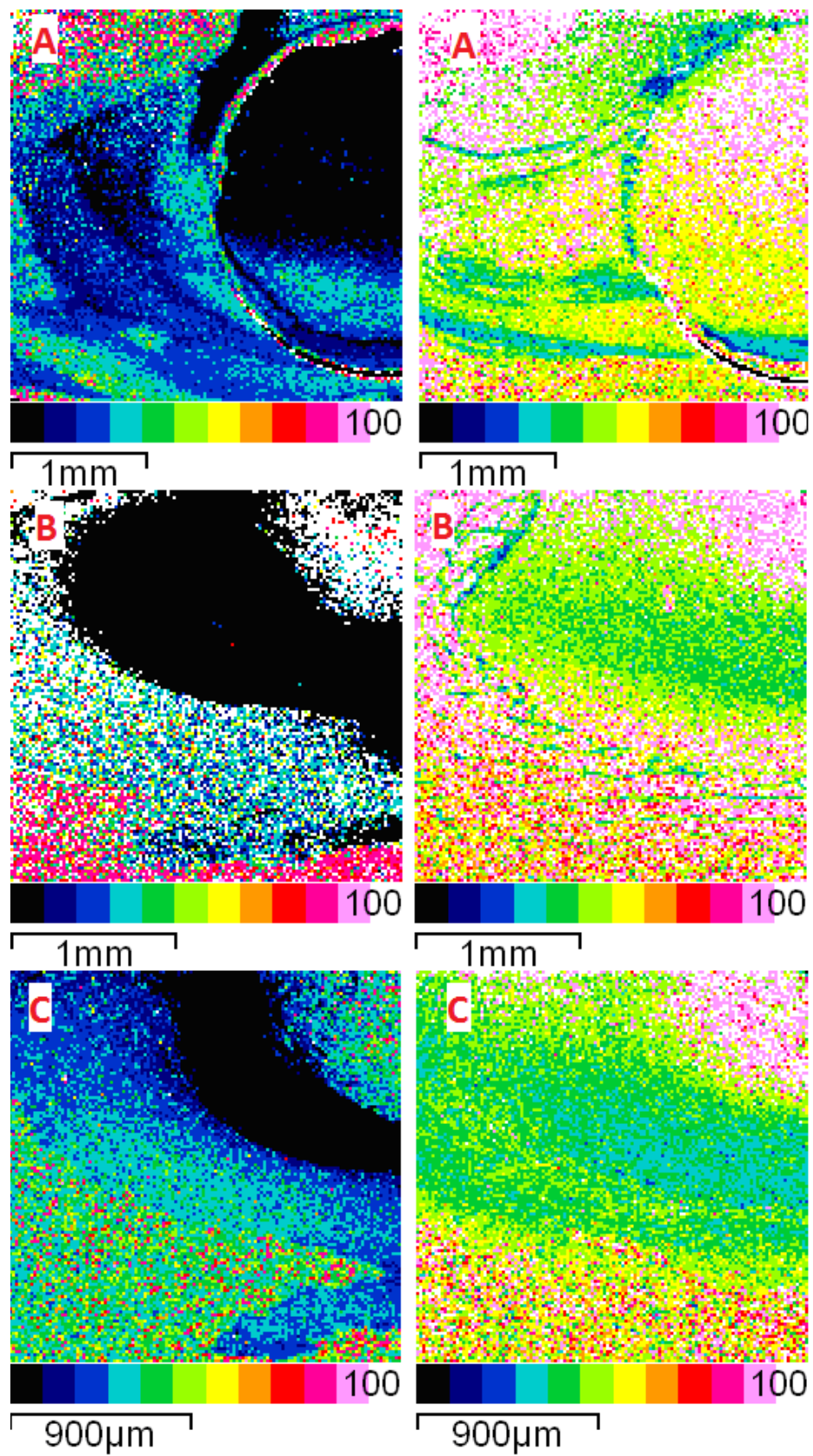


Figure 48: Quantitative X-ray of iron

Left images - Catamold® 316 Right images - PolyMIM® 316

Larger phase separation of Catamold[®] 316 is quite clear from the quantitative X-ray mapping. Catamold[®] 316 has many areas without evidence of iron. The situation is more positive in case of PolyMIM[®] 316 material.

5.3 Evaluation of separation and statistics

By the analytical computational method the concentration of some elements was measured in (128 x128) pixels windows. The goal was to find a distribution of metallic particles in a polymer binder. Iron was chosen as an indicator of particles.

The concentration of iron varying from 0 to 100 % was used for next analysis. First problem is extremely high spatial variability of iron content. In some points pure polymer with no iron was detected, in neighboring point a particle and 100 % of iron can be found. The first step of data analysis is a data smoothing. In any pixel the iron concentration is smoothed as average value of iron content of closest - usually (5x5) pixels - neighborhood of a given point. For determination of the variability of iron content two methods with similar results were suggested. The first is to approximate iron amount in some neighborhood of pixel by plane and determine its gradient as a measure of the particle distribution variability. The second method is to compute a standard deviation or a coefficient of variance of iron content in the same neighborhood of the pixel.

Unmolded samples

Table 8: Concentration of iron and variability of unmolded samples

Sample	Concentration of iron	Variability
Catamold 316_1	35.2	7.7
Catamold 316_2	33.5	5.7
Catamold 316_3	36.8	5.7
Catamold 316_4	37.5	6.6
Catamold 316_5	35.2	6.7
PolyMIM 316_1	82.3	6.3
PolyMIM 316_2	76.8	6.4
PolyMIM 316_3	82.1	3.6
PolyMIM 316_4	80.1	4.5
PolyMIM 316_5	80.9	5.8

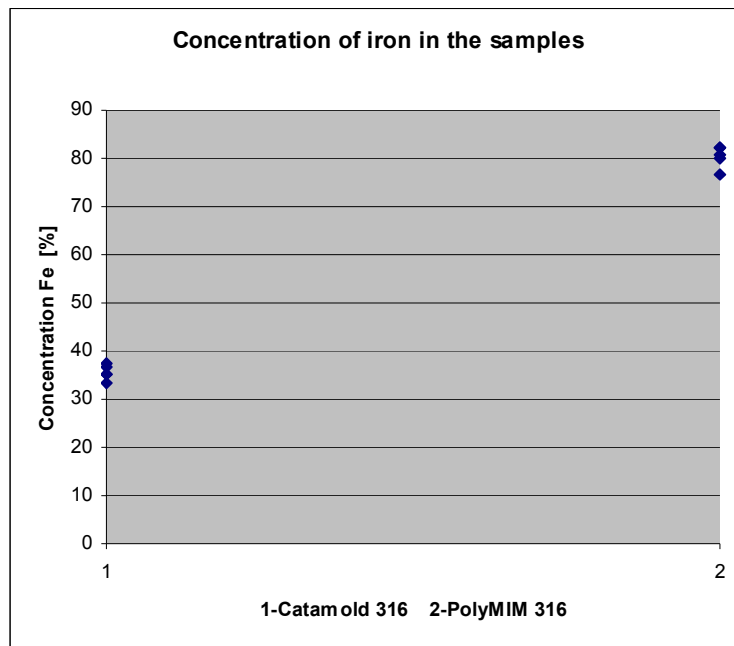


Figure 49: Concentration of iron and variability of unmolded samples

Separated samples of Catamould® 316

Table 9: Concentration of iron and variability of separated samples of Catamould® 316

Square element	Number of sample			
	1	2	3	4
A (1)	8.2	16.3	14.9	14.6
B (2)	11.1	19.2	20.9	19.9
C (3)	15.3	22.5	28.8	27.5
	Concentration of iron [%]			

Square element	Number of sample			
	1	2	3	4
A (1)	9.9	9.8	9.2	8.9
B (2)	11.7	12.4	16.5	11.4
C (3)	15.2	10.7	17.9	15.2
	Variability			

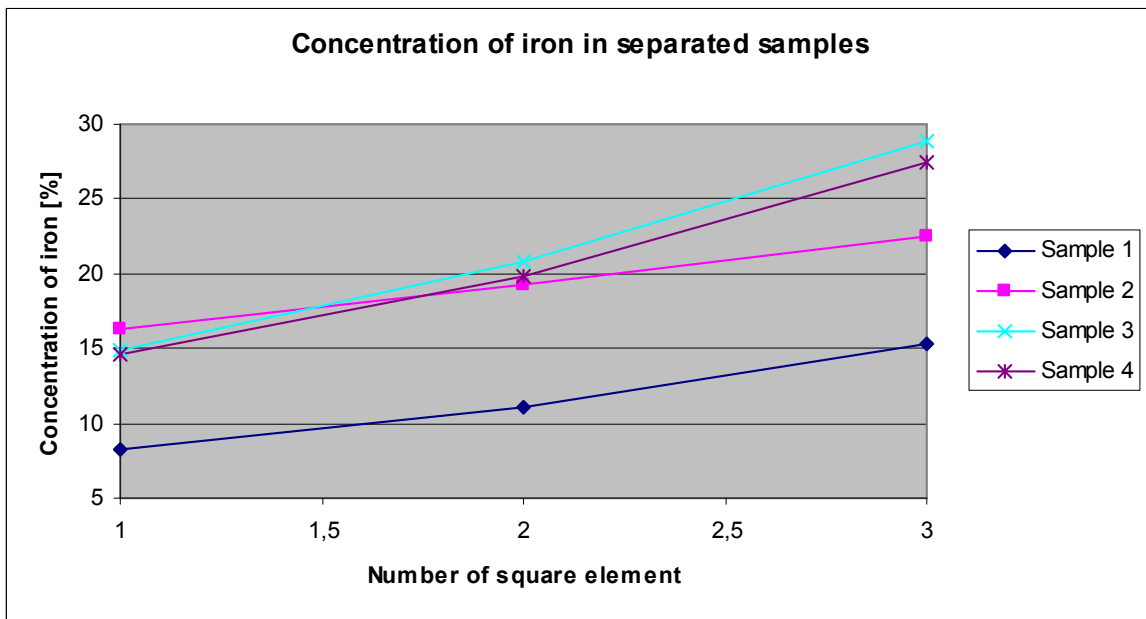


Figure 50: Concentration of iron of separated samples of Catamold[®] 316

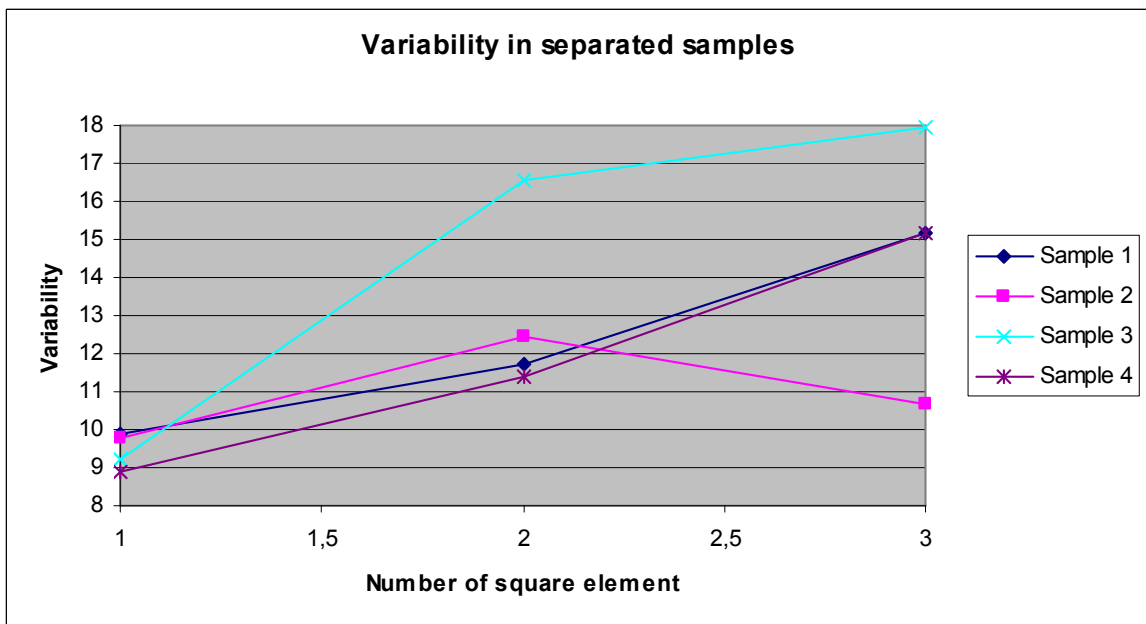


Figure 51: Variability of separated samples of Catamold[®] 316

Separated samples of PolyMIM[®] 316

Table 10: Concentration of iron and variability of separated samples of PolyMIM[®] 316

Square element	Number of sample			
	1	2	3	4
A (1)	52.6	63.6	60.7	61.3
B (2)	55.2	64.3	62.4	62.2
C (3)	48.3	51.5	53.2	51.3
Concentration of iron [%]				

Square element	Number of sample			
	1	2	3	4
A (1)	8.4	14.5	12.0	12.8
B (2)	10.0	13.4	15.0	11.8
C (3)	11.1	14.7	16.5	16.7
Variability				

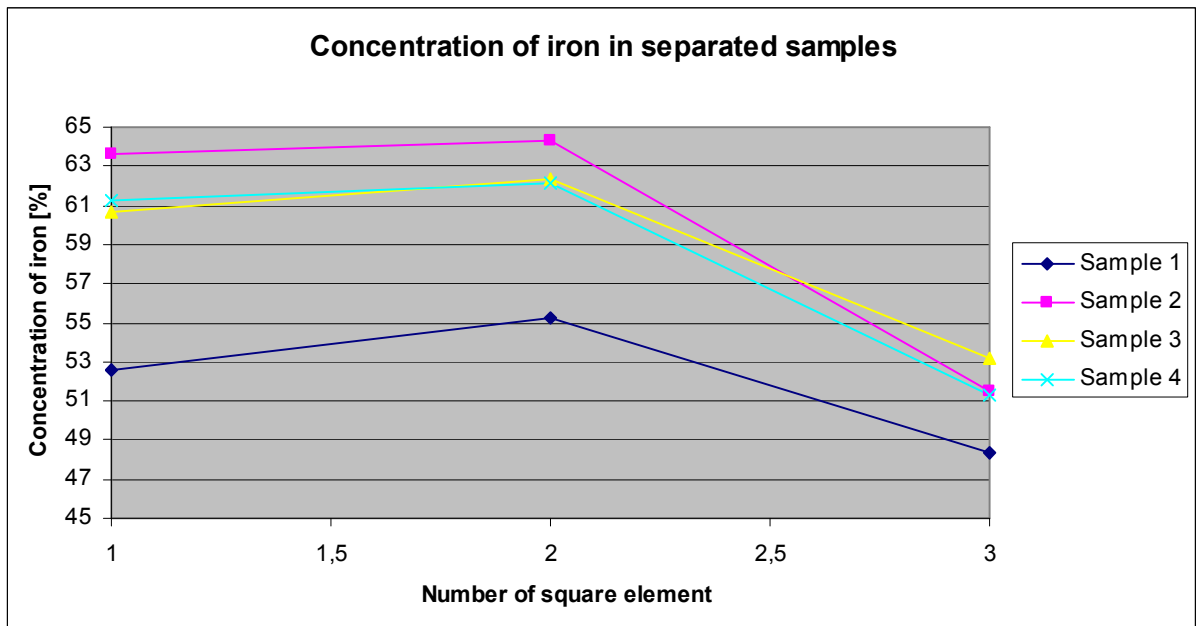


Figure 52: Concentration of iron of separated samples of PolyMIM[®] 316

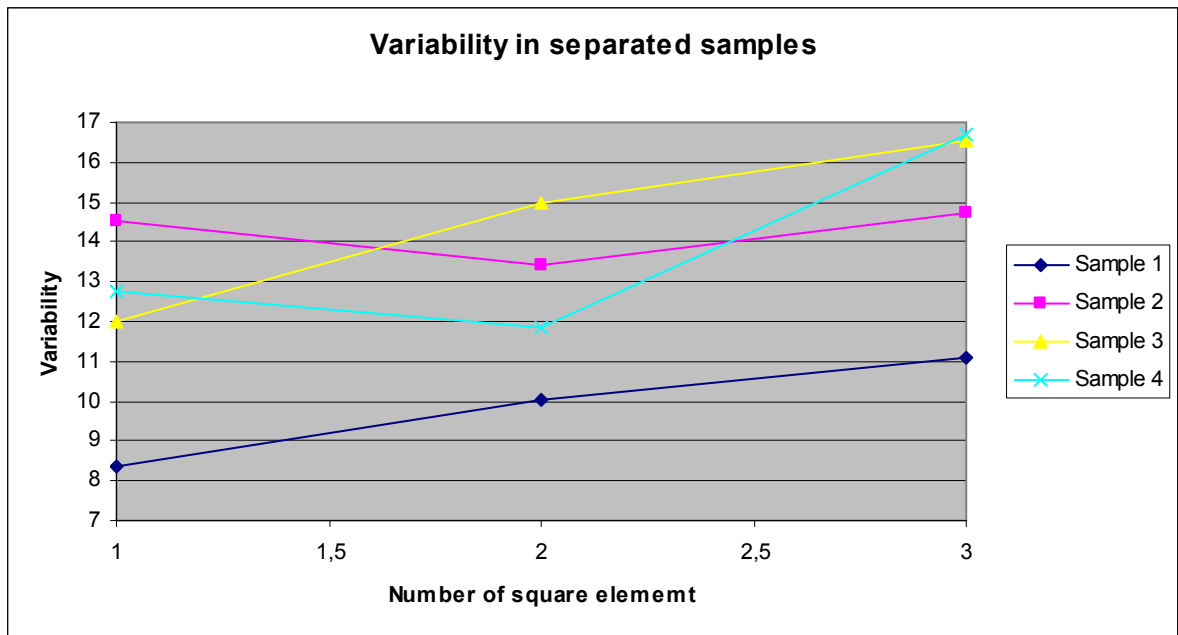


Figure 53: Variability of separated samples of PolyMIM[®] 316

Different behavior of materials is evident from the analysis. PolyMIM[®] 316 appears to be more predictable. The concentration of iron in Catamold[®] 316 unexpectedly increases from square element A to element C. On the opposite, decreasing of the concentration of iron takes PolyMIM[®] 316. Variability of PolyMIM[®] 316 is also more stable and constant in all three elements. This will ensure better predictability of the production process and less defects.

CONCLUSION

This master thesis describes PIM technology in general, its advantages and disadvantages, and also the main stages of this processing route. The theoretical part is focused on the review of research devoted to the phase separation and description of the testing mold especially designed at the TBU to depict phase separation. The phase separation is the main problem causing the defects, cracks and porosity during processing. The majority of these problems are not detected before the final step is reached. And thus, from both economic and ecological points of view, it is very important to prevent them earlier.

To study the separation, two commercially available materials were compared. The different behavior during injection molding was found. The SEM/EDX analysis showed that the feedstock Catamold[®] 316 contained an unusually large amount of manganese (data sheet of Catamold[®] 316 provides less than 2 weight %). The different behavior of materials was also confirmed with thermogravimetric analysis. Weight losses due to binder removal of both materials were different. While the PolyMIM[®] 316 carbon lost weight only 3.8 %, Catamold[®] 316 weight lost was 8 %.

Catamold[®] 316 behaves more unpredictable during injection molding in comparison to PolyMIM[®] 316. In the first step (square element A) phase separation is constant. Other square elements (B, C) exhibit more unexpected separation. This fact can cause problems during the manufacturing process. Phase separation of PolyMIM[®] 316 is more constant and due to this fact more predictable. In all square elements it remains nearly constant. Predictability of phase separation is the main condition of high-quality production without defects.

BIBLIOGRAPHY

- [1] AHN, S., PARK, S.J., LEE, S., ATRE, S., GERMAN, R.M. Effect of powders and binders on material properties and moulding parameters in iron and stainless steel powder injection moulding process. *Powder Technol.* 193 (2009), p. 162–169.
- [2] PIOTTER, V., BAUER, T., BENYLER, T., EMDE, A. Injection molding of components for Microsystems. *Microsystem Technologies* 7 (2001), p. 99-102.
- [3] HAUSNEROVÁ, B. Powder Injection Moulding – An Alternative Processing Method for Automotive Items. *Trends and Developments in Automotive Engineering*, Vienna: In Tech 2011, p. 129-149.
- [4] MPIF: *All You Need to Know about Powder Metallurgy* [online]. c2000 [cited 2011-02-12]. Accessible from: < <http://www.mpif.org>>
- [5] GERMAN, Randall M.; BOSE, Animesh. *Injection Molding of Metals and Ceramics* [s.l.] : Metal Powder Industry, 1997. 413 p. ISBN 978-1878954619
- [6] JIRÁNEK, Lukáš. *Testing mold design for investigation of powder-binder separation during powder injection molding*. Master thesis. Tomas Bata University in Zlín, Faculty of technology, 2010. 69 p.
- [7] KRUDYS, A., J., Jr.HAAKE T. Determining Formulation and Prediction Processability of “PIM” Feedstock. *Thermo Haake Material Characterization*. 2 p.
- [8] LI, Y., LI, L., Khalil, K.A. Effect of powder loading on metal injection moulding stainless steel. *Journal of Materials Processing Technology*, 183 (2-3) (2007), pp. 432–439.
- [9] HEANEY, D.F. Qualification method for powder injection molded components. *P/M Science and Technology Briefs*. Vol. 6, No.3, 2004, pp.21-27
- [10] PORTER, Marie-Aude. *Effects of Binder Systems for Metal Injection Moulding*. Master thesis Lualeå University of Technology, 2003. 80p
- [11] ADAMES, Juan M. *Characterization of Polymeric Binders for Metal Injection Molding (MIM) Process*. Dissertation thesis. University of Akron, 2007.237 p.
- [12] HAUSNEROVÁ, B. *Multi-disciplinary approach to PIM technology*. Salerno, Italy. Lifelong Learning Programme, 26.6 – 9.7.2011

- [13] SUPATI, R., LOH, N.H., KHOR, K.A., TOR, S.B. Mixing and characterization of feedstocks for powder injection molding. *Material letters*. 46 (2000), pp. 109 – 114.
- [14] *Sigma mixer*. [online]. [cited 2012-03-09]. Accessible form:
<<http://www.sigmamixer.in/>>
- [15] *ThomasNet*. [online]. [cited 2012-03-09]. Accessible form:
< <http://news.thomasnet.com/npProductsInNews.html?pncat=1303&startingat=100>>
- [16] MORITZ, T., REINHARD, L. Current status of ceramic injection moulding. *Faunhofer Institute for Ceramic Technologies and System*. 17 p.
- [17] *Rutland plastic limited*. [online]. [cited 2012-03-12]. Accessible form:
<http://www.rutlandplastics.co.uk/moulding_machine.shtml>
- [18] Powder Injection Moulding (PIM) Production of complex moulded parts from metal and ceramics. *Application information*. Arburg. 2009. 24 p.
- [19] Kinetics metal injection molding. *Design Guild*. Kinetics. 2004. 34 p.
- [20] MIM technologies, *Conference of Student creative (STČ)*; Prague. Tuma, T., Ed.; 2005.
- [21] *ESRF A Light for Science* [online]. [cited 2012-04-28]. Accessible form:
<<http://www.esrf.eu/UsersAndScience/Publications/Highlights/2002/Materials/MAT3>>
- [22] HAUSNEROVÁ, B. *Flow behavior of polymer melts - rheological models*. Polymer physics. Zlín. Tomas Bata University in Zlín, 2010
- [23] MRÁČEK, A. *Physics of fluids*. Physics I. Zlín. Tomas Bata University in Zlín, 2009
- [24] HAUSNEROVÁ, B., FILIP, P., JIRÁNEK, L., SAHA, P. Phase Separation of Highly Filled Powder/Polymer Compounds. *Mathematical Methods and Techniques in Engineering and Environmental Science*. pp. 257 – 260. ISBN: 978-1-61804-046-6
- [25] Mannschatz, A., Höhn, S., Moritz, T. Powder-binder separation in injection moulded green parts, *Journal of the European Ceramic Society*, Volume 30, Issue 14, October 2010, Pages 2827-2832, ISSN 0955-2219
- [26] *Purdue university, Radiological and Environmental Management*. [online]. [cited 2012-05-02]. Accessible form:
< <http://www.purdue.edu/rem/rs/sem.htm>>

LIST OF ABBREVIATIONS

2D	Two dimensional
3D	Three dimensional
BSE	Backscattered electron detector
CIM	Ceramic injection molding
DSC	Differential scanning calorimetry
DTG	Differential thermogravimetry
MIM	Metal injection molding
PE	Polyethylene
PEG	Polyethylene glycol
PIM	Powder injection molding
PMMA	Polymethyl methacrylate
POM	Polyoxymethylene
PP	Polypropylene
PS	Polystyrene
PVA	Polyvinyl alcohol
®	Registered trademark
SE	Secondary electron detector
SEM	Scanning electron microscopy
TEM	Transmission electron microscopy
TGA	Thermogravimetric analysis

LIST OF FIGURES

<i>Figure 1: MIM diesel turbocharger vane for automotive manufactured</i>	12
<i>Figure 2: Automotive engine stator [4]</i>	13
<i>Figure 3: Stainless steel bobbins [4]</i>	14
<i>Figure 4: Stainless steel lock parts [4]</i>	14
<i>Figure 5: Hearing aid receiver can [4]</i>	15
<i>Figure 6 : Orthodontic bracket [4]</i>	15
<i>Figure 7: Three possible situations of powder:binder ratio in a feedstock;</i>	16
<i>Figure 8: SEM of a feedstock used in PIM</i>	19
<i>Figure 9: Polymer binders [12]</i>	20
<i>Figure 10: Schematic diagram of PIM [6]</i>	22
<i>Figure 11: A batch mixing: (a) planetary mixer; (b) Z-blade mixer [14, 15]</i>	23
<i>Figure 12: Injection molding machine [17]</i>	24
<i>Figure 13: Scheme of a molding cycle [18]</i>	25
<i>Figure 14 : Course of thermal debinding [5]</i>	26
<i>Figure 15: Sintering process</i>	30
<i>Figure 16 : Basic rheological model [22]</i>	32
<i>Figure 17: Viscosity dependence on the solids loading [5]</i>	34
<i>Figure 18: Particles of powder with mobile and immobile binder. [5]</i>	34
<i>Figure 19: Capillary rheometer – homogenous and inhomogeneous feedstock [11]</i>	35
<i>Figure 20: Torque rheometer – homogenous and inhomogeneous feedstock [11]</i>	36
<i>Figure 21: Phase separation - effect of shear rate gradient [3]</i>	37
<i>Figure 22: Schematic diagram of defects during entire molding process [5]</i>	37
<i>Figure 23: Molding defects [5]</i>	38
<i>Figure 24: Origin of a fountain flow [5]</i>	39
<i>Figure 25: Moldability testing molds [27]</i>	39
<i>Figure 26 : 2D distribution of the powder in the corner of the square spiral mold.</i> <i>a - balance model, b - DSC, c - tomography, d - radiography [6]</i>	40
<i>Figure 27 : 3D distribution of the powder in the corner of the square spiral mold.</i> <i>a - balance model, b - DSC [6]</i>	41
<i>Figure 28: Testing mold [3]</i>	41
<i>Figure 29 : SEM of phase separation [6]</i>	42

<i>Figure 30: Arburg Allrounder 370S</i>	45
<i>Figure 31: Injection molded testing samples: a - short shot, b - optimized.</i>	48
<i>Figure 32: Scheme of scanning electron microscope</i>	49
<i>Figure 33: SEM of unmolded Catamold[®] 316 feedstock</i>	50
<i>Figure 34: SEM of unmolded PolyMIM[®] 316 feedstock</i>	51
<i>Figure 35: TGA of Catamold[®] 316 on air</i>	52
<i>Figure 36: TGA of PolyMIM[®] 316 on air</i>	52
<i>Figure 37: Locations scanned with SEM [6]</i>	53
<i>Figure 38: Phase separation located at the gates to the particular testing</i>	54
<i>Figure 39: Sum spectrum of Catamold[®] 316</i>	55
<i>Figure 40: EDX of Catamold[®] 316</i>	56
<i>Figure 41: Sum spectrum of PolyMIM[®] 316</i>	56
<i>Figure 42: EDX of PolyMIM[®] 316</i>	57
<i>Figure 43: Sum spectra of separated samples of Catamold[®] 316</i>	58
<i>Figure 44: Sum spectra of separated samples of PolyMIM[®] 316</i>	59
<i>Figure 45: EDX of carbon.</i>	60
<i>Figure 46: EDX of iron.</i>	61
<i>Figure 47: Quantitative X-ray of carbon</i>	62
<i>Figure 48: Quantitative X-ray of iron</i>	63
<i>Figure 49: Concentration of iron and variability of unmolded samples</i>	65
<i>Figure 50: Concentration of iron of separated samples of Catamold[®] 316</i>	66
<i>Figure 51: Variability of separated samples of Catamold[®] 316</i>	66
<i>Figure 52: Concentration of iron of separated samples of PolyMIM[®] 316</i>	67
<i>Figure 53: Variability of separated samples of PolyMIM[®] 316</i>	68

LIST OF TABLES

Table 1: Examples of PIM powders [9]	18
Table 2: Comparison of debinding techniques and times [5]	29
Table 3: Mathematic models of rheological behaviors	33
Table 4: Technical data for Arburg Allrounder 370S	45
Table 5: Properties of PolyMIM [®] 316L	46
Table 6: Properties of Catamold [®] 316L	47
Table 7: Optimized molding conditions.....	48
Table 8: Concentration of iron and variability of unmolded samples.....	64
Table 9: Concentration of iron and variability of separated samples of Catamold [®] 316.....	65
Table 10: Concentration of iron and variability of separated samples of PolyMIM [®] 316.....	67